Analyticity of the Scattering Amplitude and Resonance Parameters in the Meson Exchange Picture

M. Döring

in collaboration with **C. Hanhart, F. Huang, S. Krewald, U.-G. Meißner, K. Nakayama**,
Forschungszentrum Jülich, University of Georgia, Universität Bonn

Nucl. Phys. A **829**, 170 (2009), Phys. Lett. B **681**, 26 (2009)

The Jülich model of pion-nucleon interaction

- Analytic coupled channel model based on meson exchange (chiral Lagrangian of Wess and Zumino).
- Channels πN, ηN; effective $\pi\pi N$ channels σN, ρN, $\pi\Delta$.
- Baryonic resonances up to $J = 3/2$ with derivative couplings as required by chiral symmetry.
- References: Schütz PRC 51 (1995), Krehl PRC 62 (2000), Gasparyan PRC 68 (2003), Döring NPA 829 (2009).

  Other meson exchange models: Sato, Lee, PRC 54 (1996); Surya, Gross, PRC 53 (1996); Juliá Díaz et al., PRC 76 (2007); Suzuki, Sato, Lee, PRC 79 (2009); Kamano et al., PRC 80 (2009); Kamano et al., PRC 79 (2009).

Scattering equation in the JLS basis

Scattering equation guarantees two-body unitarity: T=V+VGT

$$\langle L'S'k'|T^{IJ}_{\mu\nu}|LSk\rangle = \langle L'S'k'|V^{IJ}_{\mu\nu}|LSk\rangle$$
$$+ \sum_{\gamma,L''S''} \int_0^\infty k''^2\, dk'' \langle L'S'k'|V^{IJ}_{\mu\gamma}|L''S''k''\rangle \frac{1}{Z - E_\gamma(k'') + i\epsilon} \langle L''S''k''|T^{IJ}_{\gamma\nu}|LSk\rangle$$

T: Amplitude V: Pseudopotential G: Propagator

J: total angular momentum
L: orbital angular momentum
S: total Spin of MB system
I: isospin
$k(k', k'')$: incoming(outgoing, intermediate) momentum, on- or off-shell
$\mu(\nu, \gamma)$: incoming(outgoing, intermediate) channel $[\pi N, \eta N, \pi\Delta, \rho N, \sigma N]$

Partial waves in $\pi N \longrightarrow \pi N$

Data: GWU/SAID analysis, single energy solution

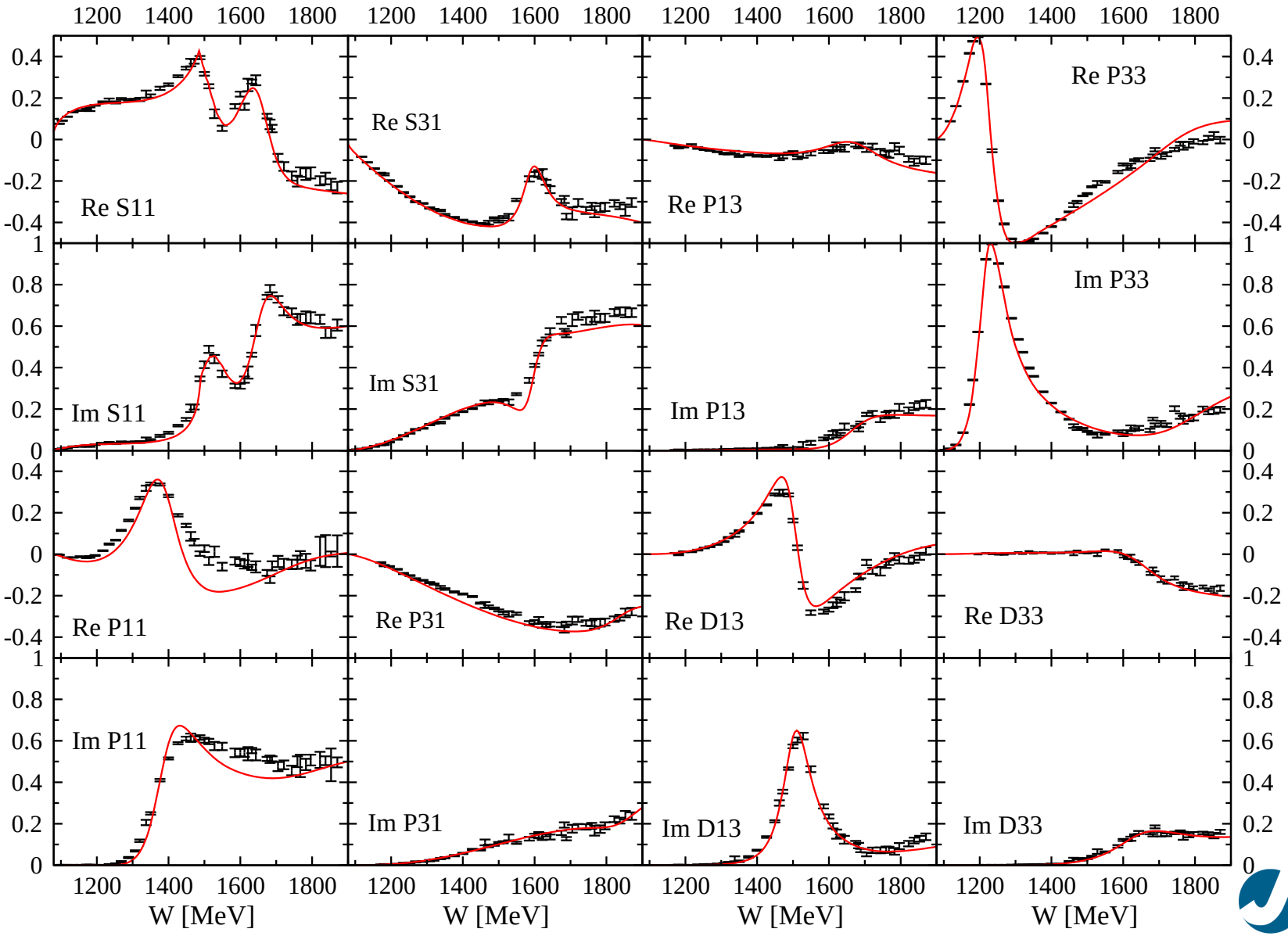

Partial waves in $\pi N \longrightarrow \pi N$

Data: GWU/SAID analysis, single energy solution

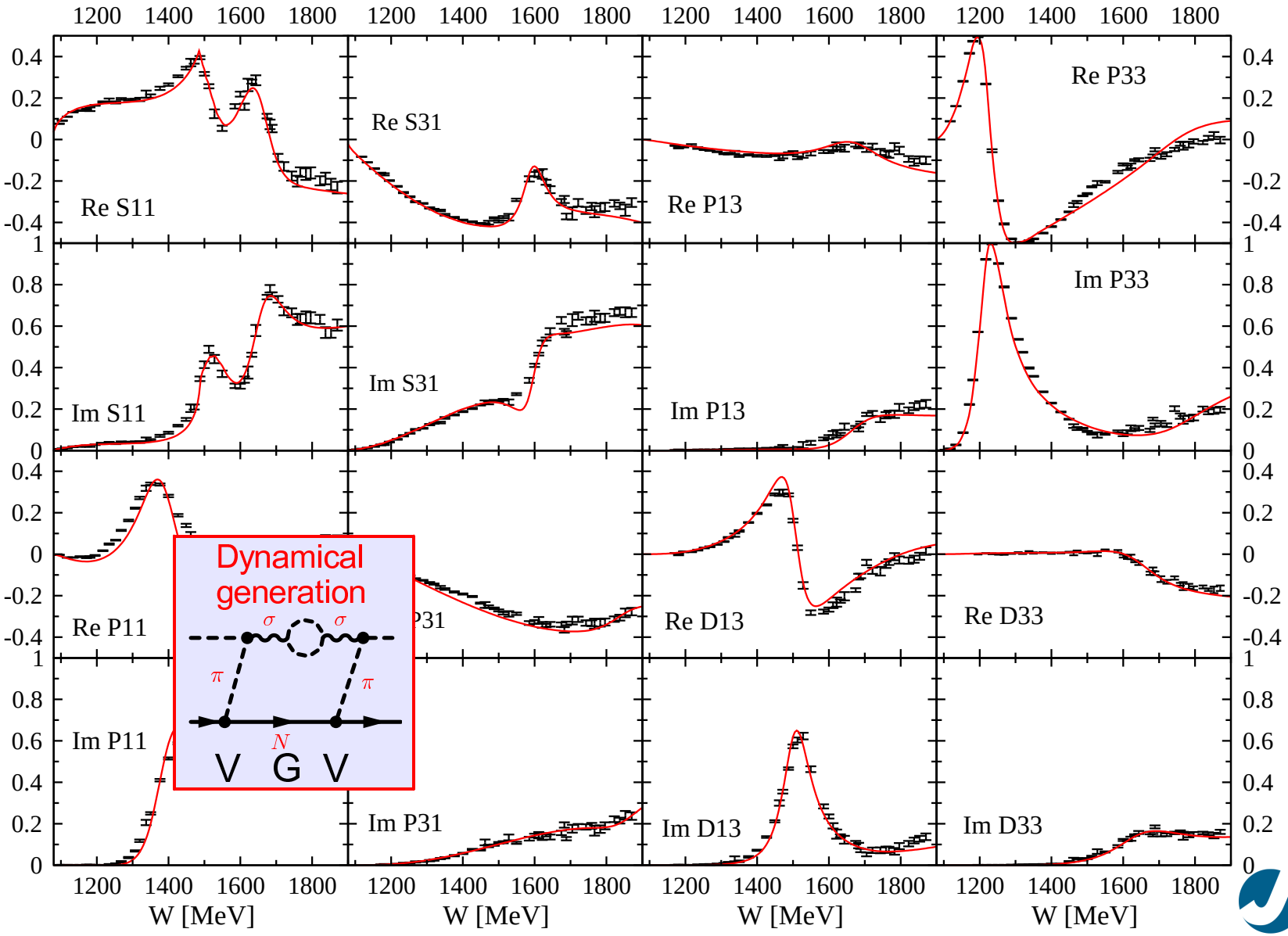

Coupled channels and gauge invariance

Haberzettl, PRC56 (1997), Haberzettl, Nakayama, Krewald, PRC74 (2006)

Hadronic scattering:

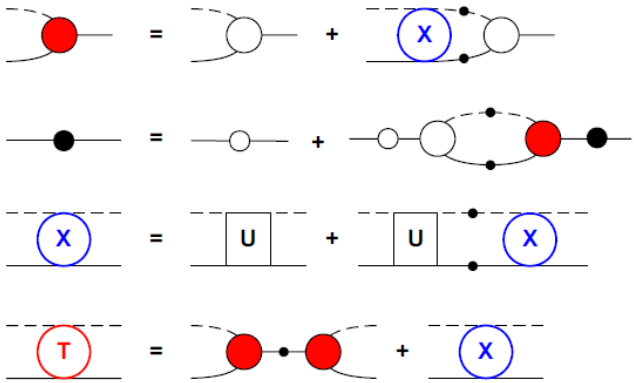

Photo-production:

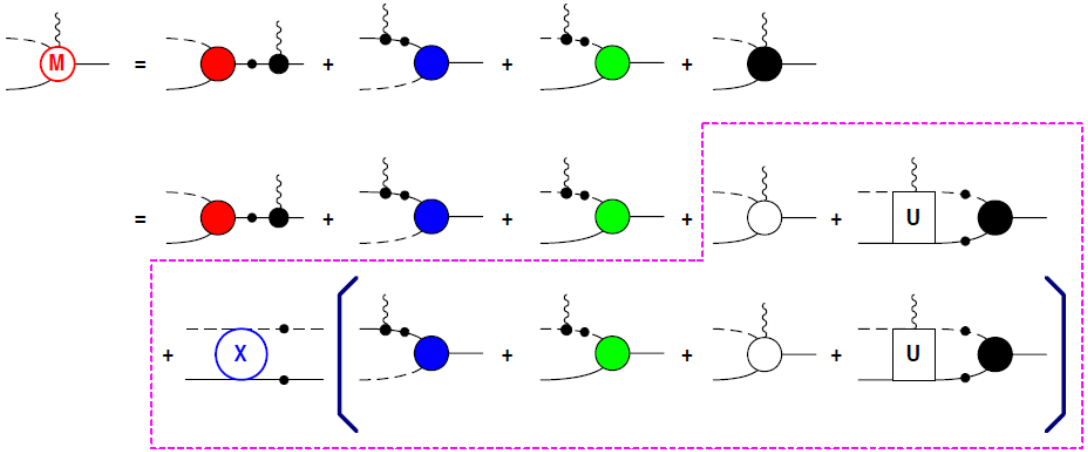

Gauge invariance: Generalized Ward-Takahashi identity (WTI)

(Note the condition of current conservation $k_\mu M^\mu = 0$ is necessary but not sufficient!)

$$k_\mu M^\mu = -|F_s\tau\rangle S_{p+k} Q_i S_p^{-1} + S_{p'}^{-1} Q_f S_{p'-k} |F_u\tau\rangle + \Delta^{-1}_{p-p'+k} Q_\pi \Delta_{p-p'} |F_t\tau\rangle$$

Strategy: Replace 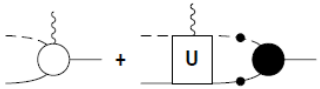 by phenomenological contact term such that the generalized WTI is satisfied

$d\sigma/d\Omega$ and Σ_γ for $\gamma p \longrightarrow \pi^+ n$

preliminary (F. Huang, K. Nakayama)

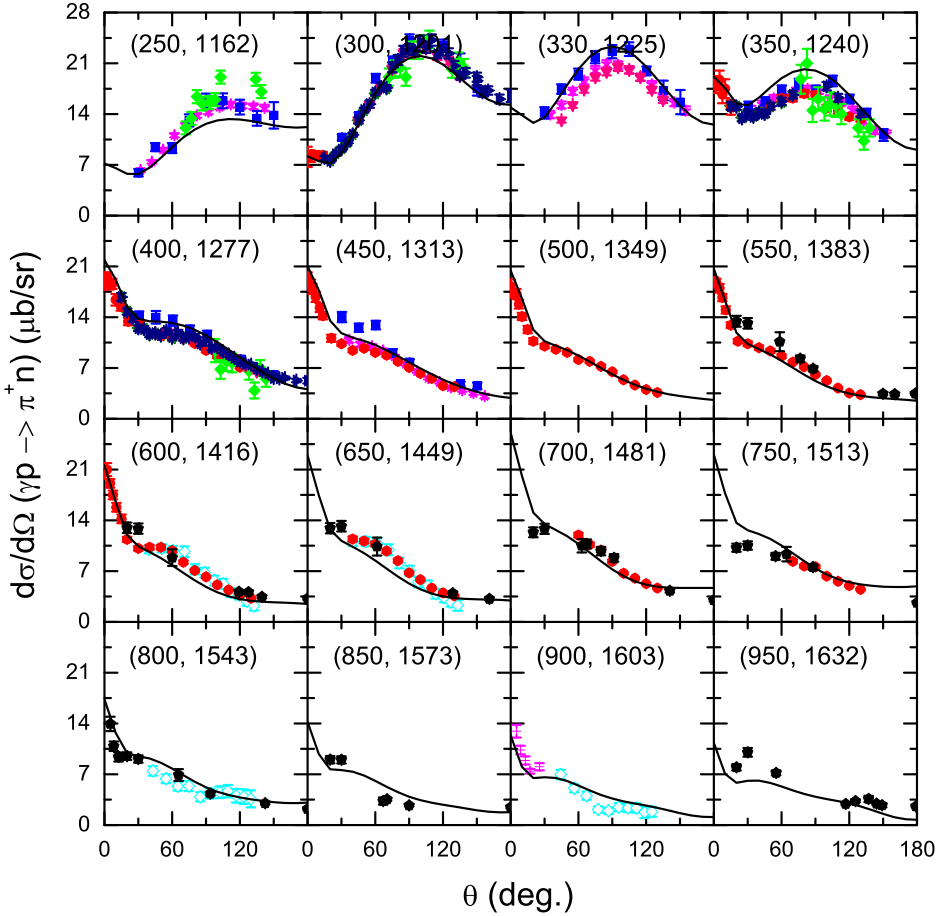

Differential cross section for $\gamma p \longrightarrow \pi^+ n$

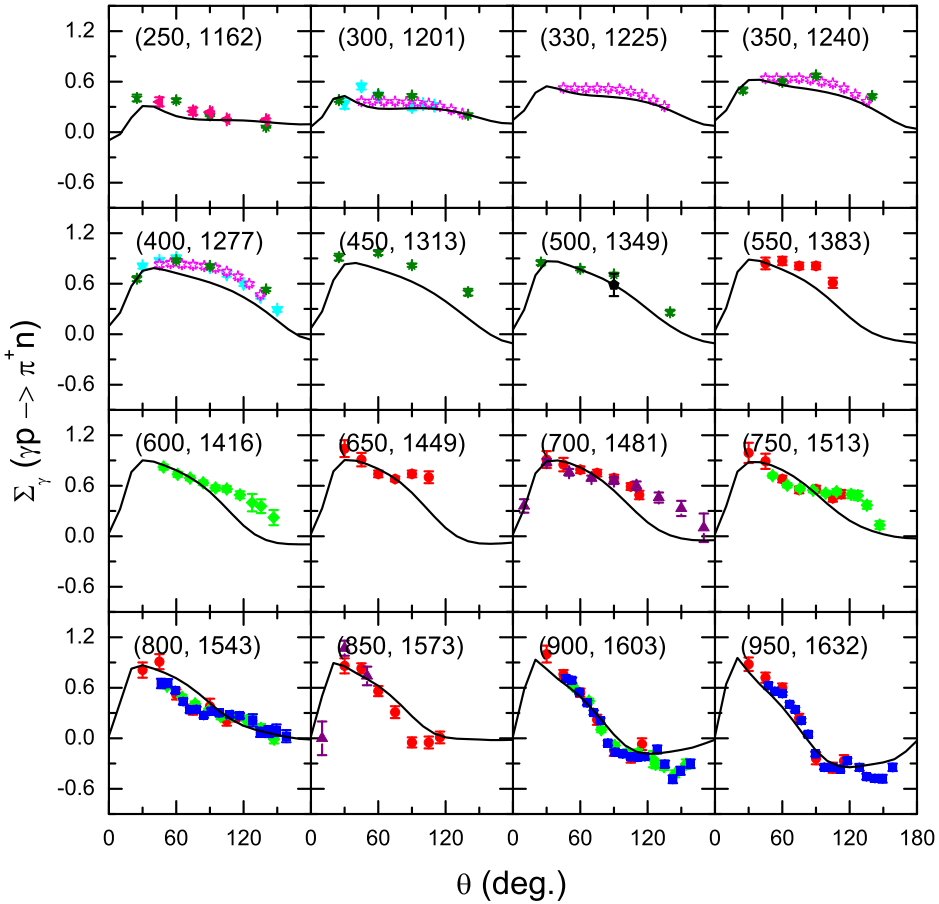

Photon spin asymmetry for $\gamma p \longrightarrow \pi^+ n$

$d\sigma/d\Omega$ and Σ_γ for $\gamma n \longrightarrow \pi^- p$

preliminary (F. Huang, K. Nakayama)

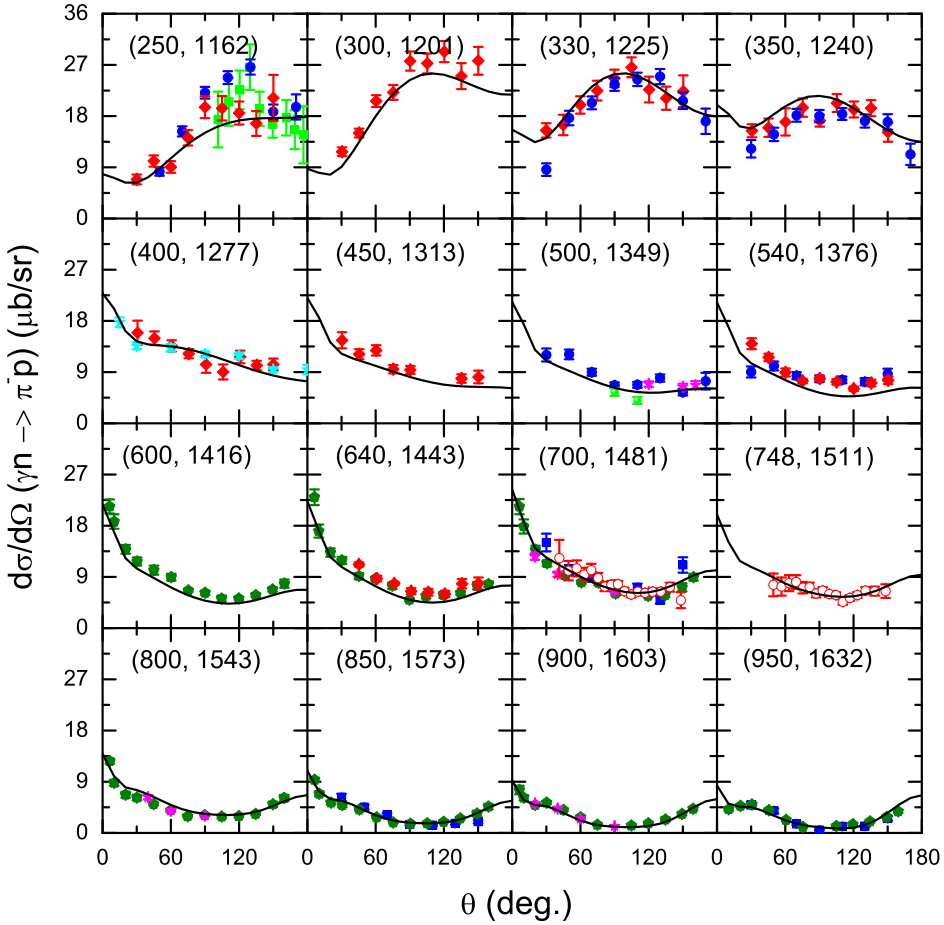

Differential cross section for $\gamma n \longrightarrow \pi^- p$

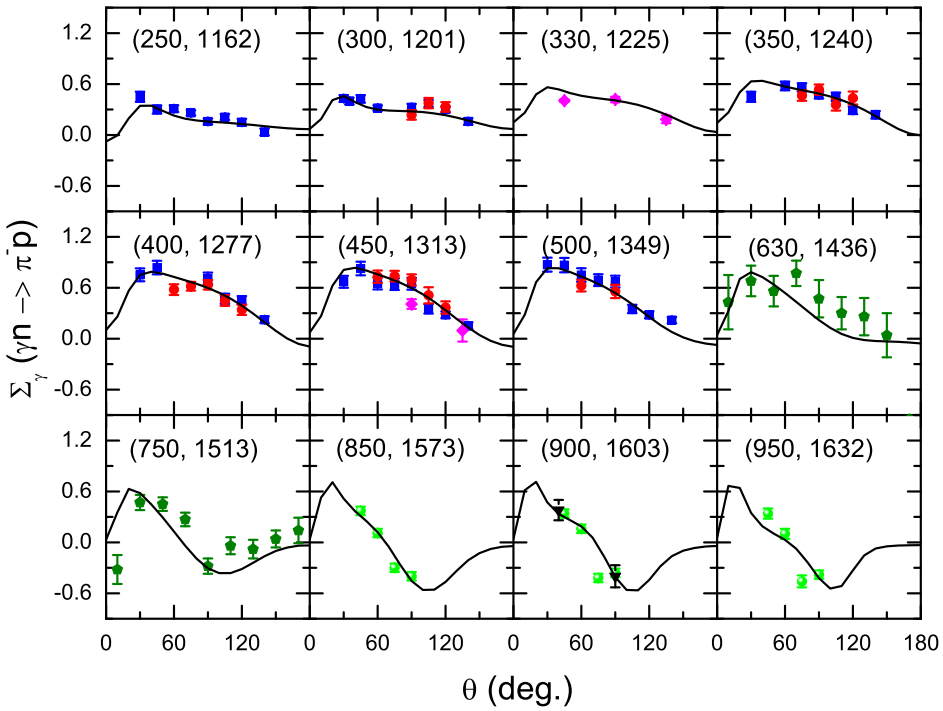

Photon spin asymmetry for $\gamma n \longrightarrow \pi^- p$

$d\sigma/d\Omega$ and Σ_γ for $\gamma p \longrightarrow \pi^0 p$

preliminary (F. Huang, K. Nakayama)

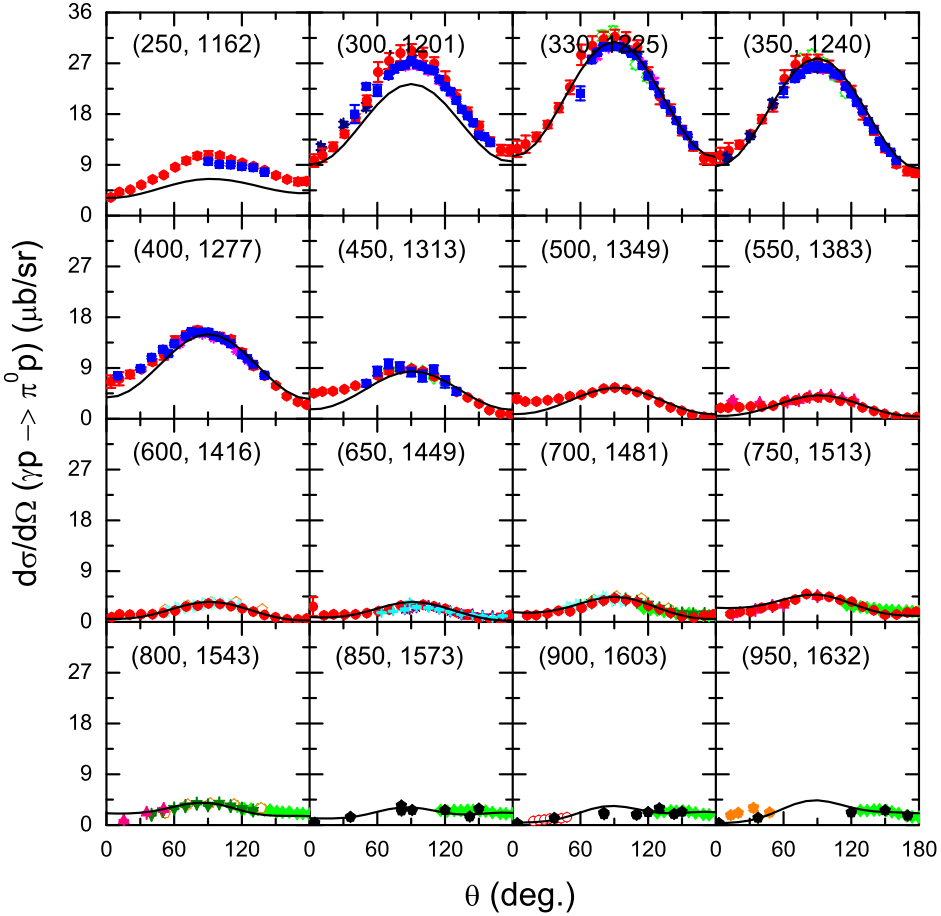

Differential cross section for $\gamma p \longrightarrow \pi^0 p$

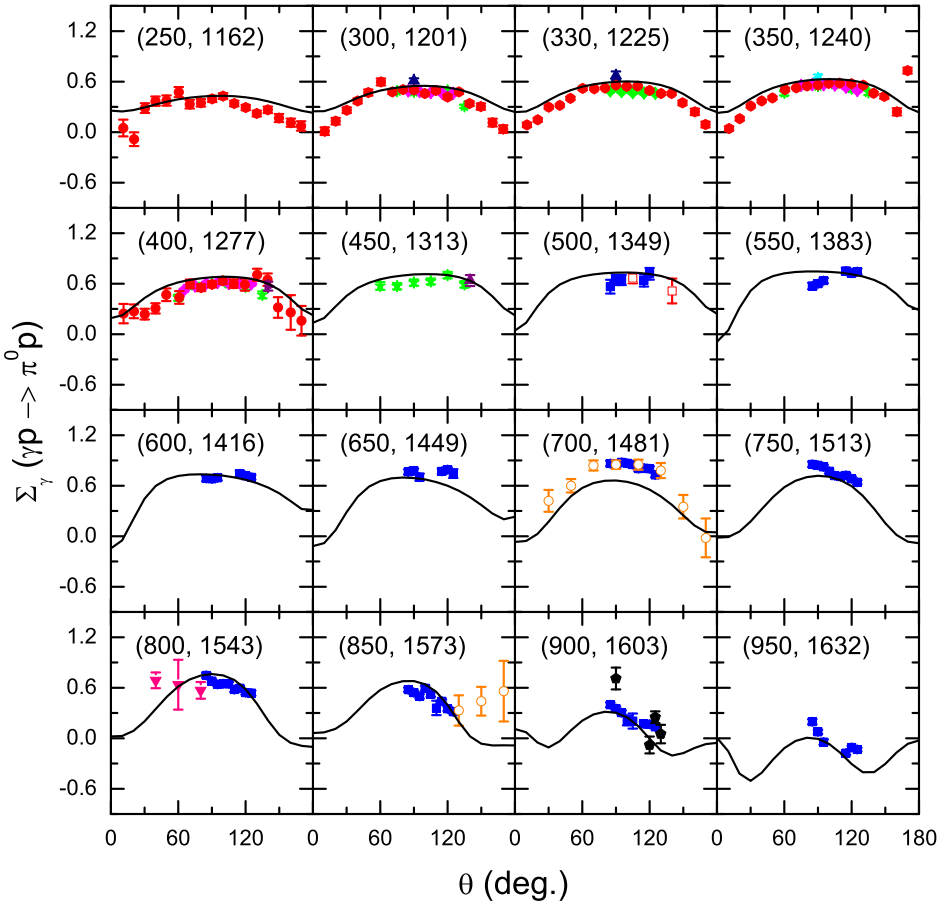

Photon spin asymmetry for $\gamma p \longrightarrow \pi^0 p$

Coupled channel effects in photo- & electro-production

Dynamically generated resonances

- Next task: Evaluate the Roper transition form factor!
- Example: the $N^*(1535)$ as a dynamically generated resonance:
  [D. Jido, E. Oset, M.D., PRC77 (2008)]

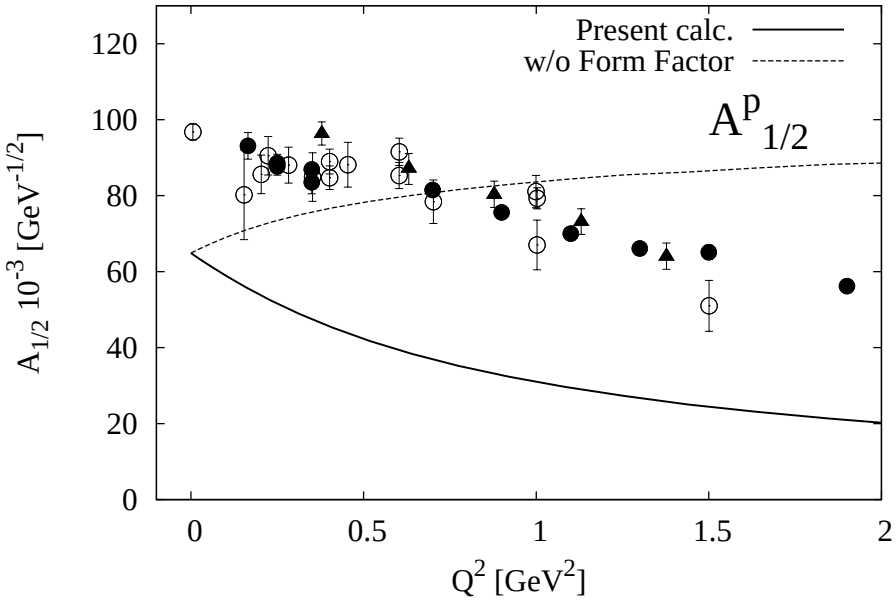

Data: JLab

- Predictions possible.

- Coupled channel effects in $\gamma N \longrightarrow \eta N$
  [M.D., K. Nakayama, EPJA43 (2010), PLB683 (2010)]

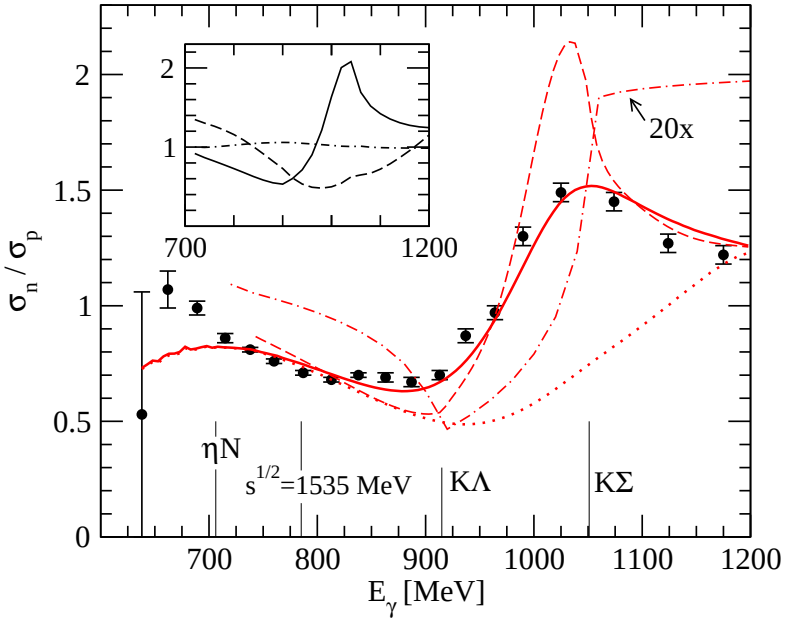

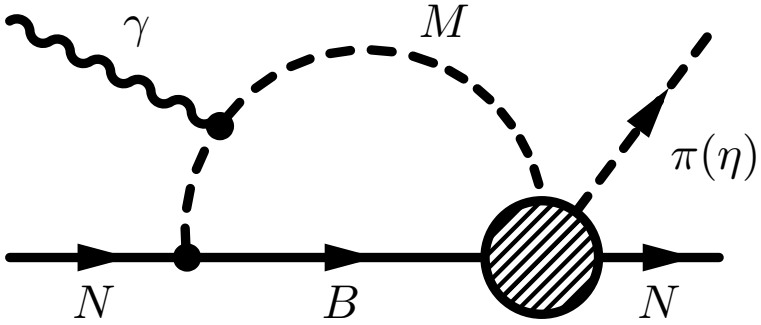

- $MB = \pi N,\ \eta N, K\Lambda, K\Sigma$

Coupled channel effects in photo- & electro-production

Dynamically generated resonances

- Next task: Evaluate the Roper transition form factor!
- Example: the $N^*(1535)$ as a dynamically generated resonance:
  [D. Jido, E. Oset, M.D., PRC77 (2008)]

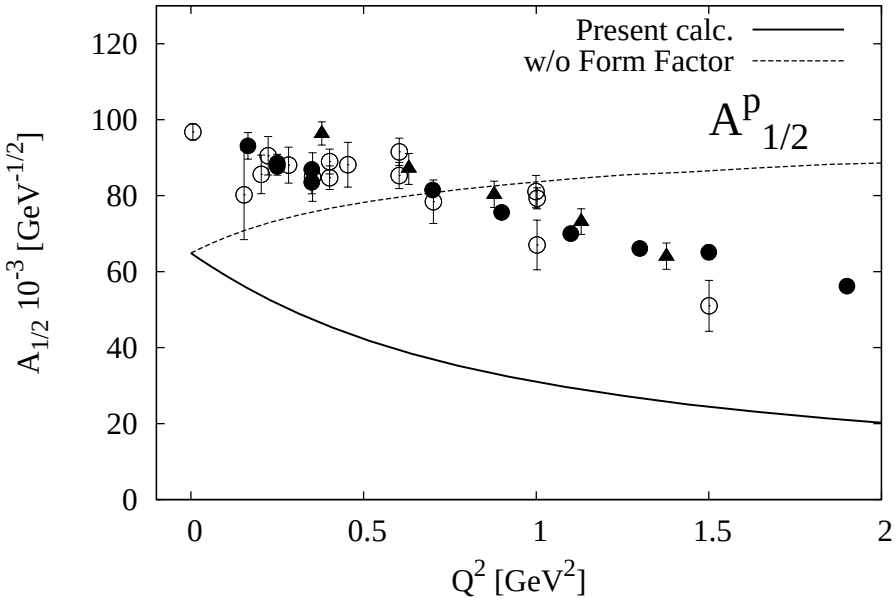

Data: JLab

- Predictions possible.

- Coupled channel effects in $\gamma N \longrightarrow \eta N$
  [M.D., K. Nakayama, EPJA43 (2010), PLB683 (2010)]

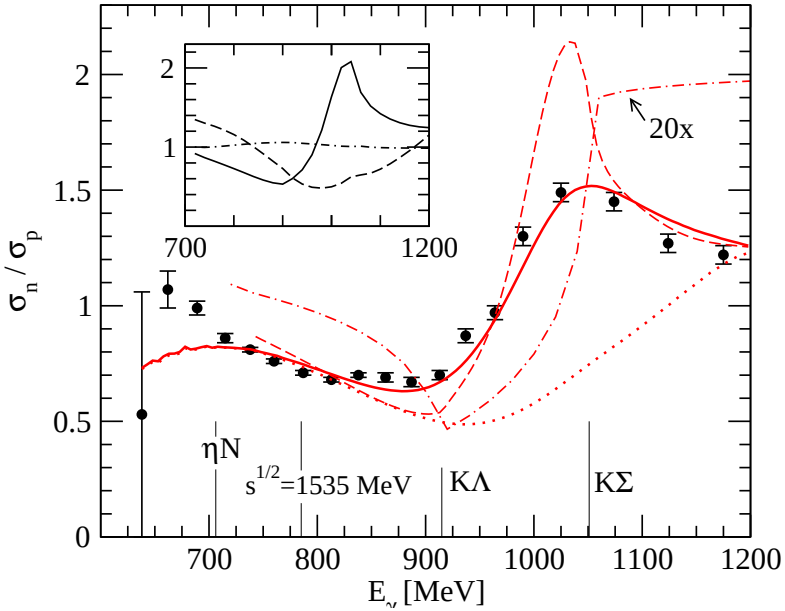

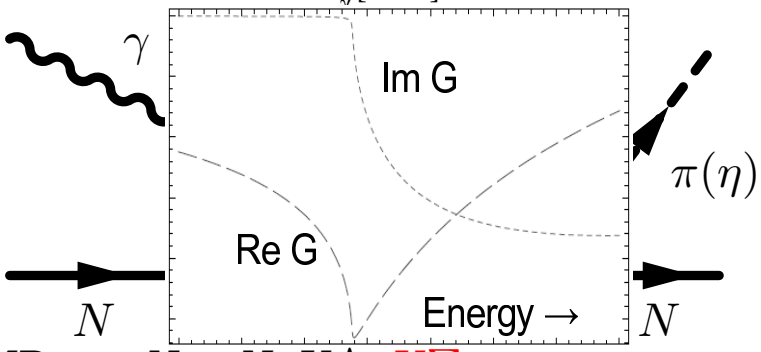

- $MB = \pi N,\ \eta N, K\Lambda, K\Sigma$

Propagator of stable particles $\pi\pi$, πN, ηN (c.m. system)

$$\Pi_\sigma(z) = \int_0^\infty q^2 dq \, \frac{(v^{\sigma\pi\pi}(q,z))^2}{z - E_1 - E_2 + i\epsilon}$$

$$E_{1,2} = \sqrt{m_{1,2}^2 + q^2}$$

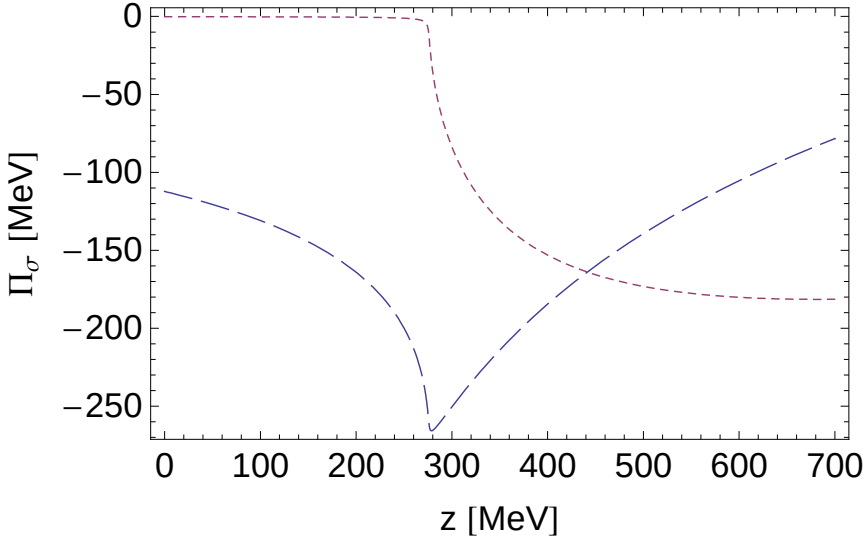

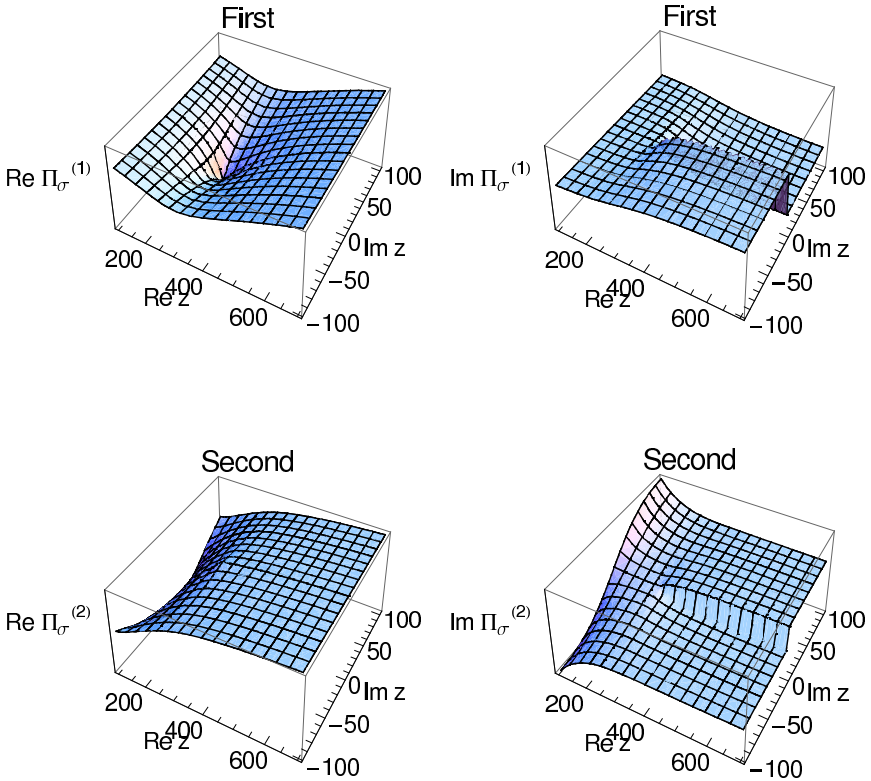

→ Righthand cut, two sheets, and one branch point!

Contour deformation

...enables access to both Riemann sheets

$$\Pi_\sigma(z) = \int_0^\infty q^2 dq \, \frac{(v^{\sigma\pi\pi}(q))^2}{z - E_1 - E_2 + i\epsilon}$$

$$z - E_1 - E_2 = 0 \Leftrightarrow q = q_{c.m.}$$

$$q_{c.m.} = \frac{1}{2z}\sqrt{[z^2 - (m_1 - m_2)^2][z^2 - (m_1 + m_2)^2]}$$

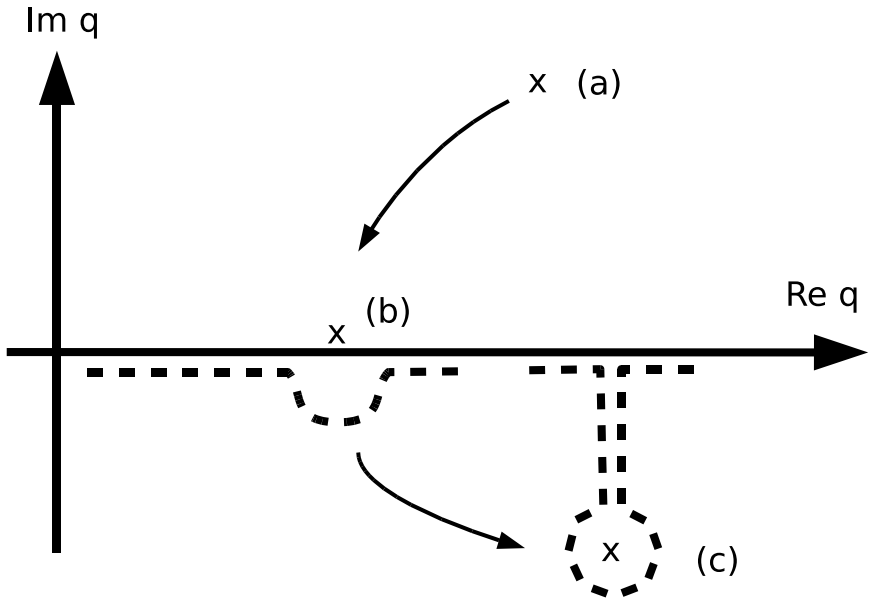

- Plot $q_{c.m.}(z)$ in the q plane of integration (X: Pole positions).
- case (a), Im $z > 0$: straight integration from $q = 0$ to $q = \infty$.
- case (b), Im $z = 0$: Pole is on real q axis.
- case (c), Im $z < 0$: Deformation gives analytic continuation.
- Special case: Pole at $q = 0$ $\Leftrightarrow$ branch point at $z = m_1 + m_2$ (= threshold).

Effective $\pi\pi N$ channels: Analytic structure

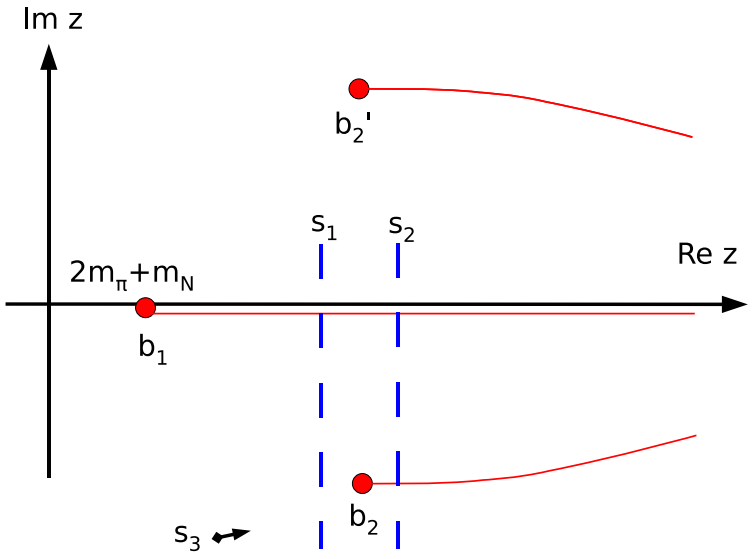

Three branch points and four sheets for each of the σN, ρN, and $\pi\Delta$ propagators.

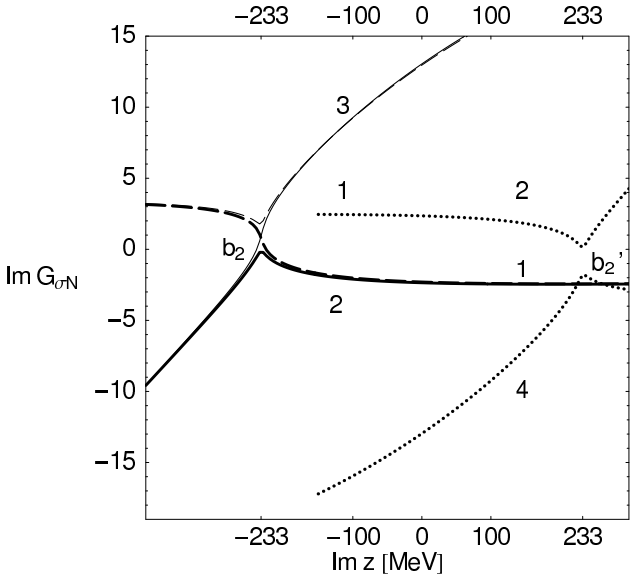

- The cut along Im $z = 0$ is induced by the cut of the self energy of the unstable particle.
- The poles of the unstable particle (σ) induce branch points in the σN propagator at

$$z_{b_2} = m_N + z_0,\ z_{b_2'} = m_N + z_0^*$$

Effective $\pi\pi N$ channels: Analytic structure

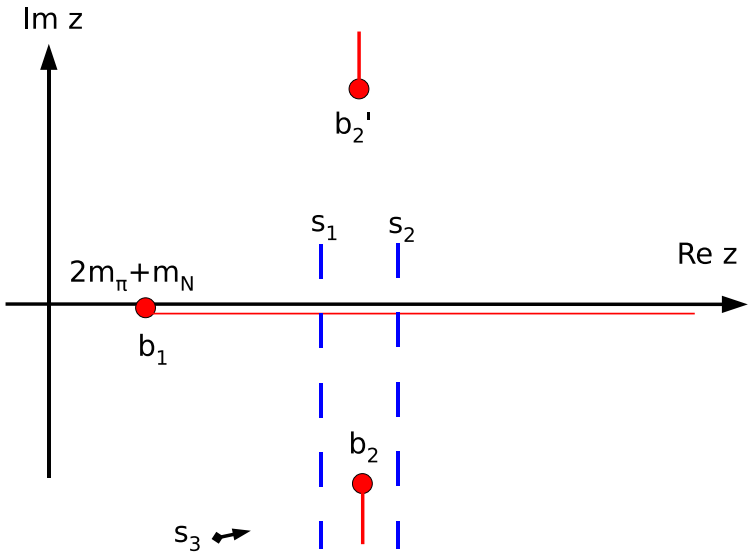

- The cut along Im $z = 0$ is induced by the cut of the self energy of the unstable particle.
- The poles of the unstable particle (σ) induce branch points in the σN propagator at

$$z_{b_2} = m_N + z_0,\ z_{b_2'} = m_N + z_0^*$$

Three branch points and four sheets for each of the σN, ρN, and $\pi\Delta$ propagators.

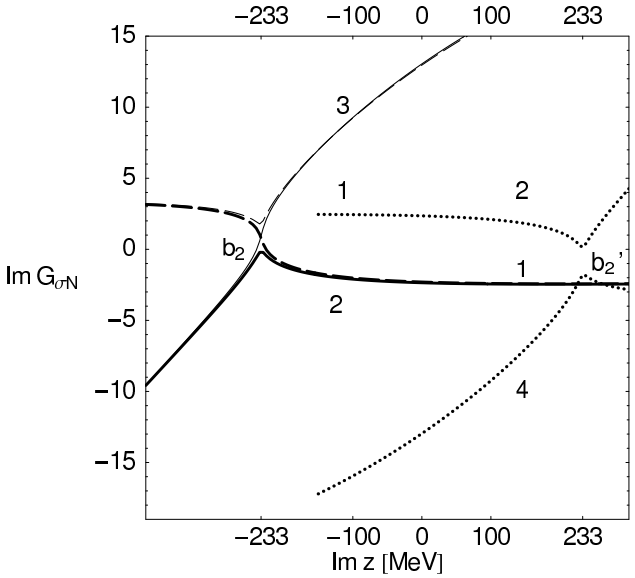

Pole search

on the unphysical sheets, given by the analytic continuation.

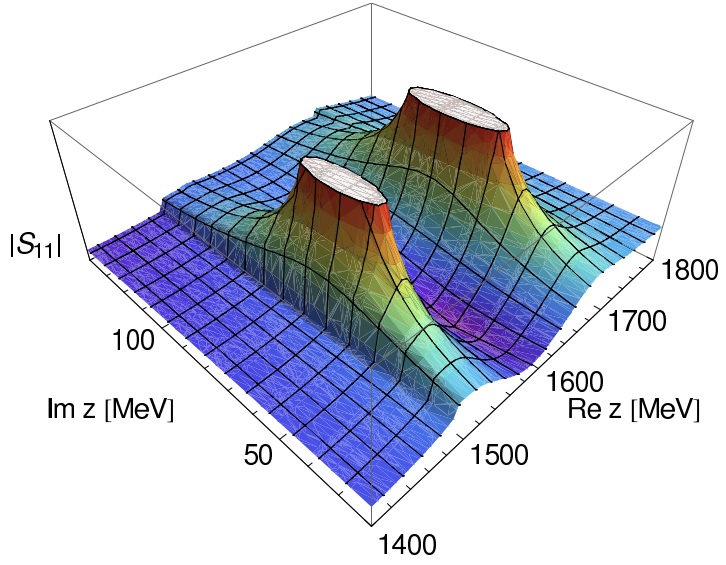

	Re z_0 [MeV]	-2 Im z_0 [MeV]	$\|R\|$ [MeV]	θ [deg] [^{0}]
$N^*(1440)\ P_{11}$	1387	147	48	-64
ARN	1359	162	38	-98
HOE	1385	164	40	
CUT	1375$\pm$30	180$\pm$40	52$\pm$5	-100$\pm$35
$N^*(1520)\ D_{13}$	1505	95	32	-18
ARN	1515	113	38	-5
HOE	1510	120	32	-8
CUT	1510$\pm$5	114$\pm$10	35$\pm$2	-12$\pm$5

	Re z_0 [MeV]	-2 Im z_0 [MeV]	$\|R\|$ [MeV]	θ [deg] [^{0}]
$N^*(1535)\ S_{11}$	1519	129	31	-3
ARN	1502	95	16	-16
HOE	1487			
CUT	1510$\pm$50	260$\pm$80	120$\pm$40	+15$\pm$45
$N^*(1650)\ S_{11}$	1669	136	54	-44
ARN	1648	80	14	-69
HOE	1670	163	39	-37
CUT	1640$\pm$20	150$\pm$30	60$\pm$10	-75$\pm$25
$N^*(1720)\ P_{13}$	1663	212	14	-82
ARN	1666	355	25	-94
HOE	1686	187	15	
CUT	1680$\pm$30	120$\pm$40	8$\pm$12	-160$\pm$30
$\Delta(1232)\ P_{33}$	1218	90	47	-37
ARN	1211	99	52	-47
HOE	1209	100	50	-48
CUT	1210$\pm$1	100$\pm$2	53$\pm$2	-47$\pm$1
$\Delta^*(1620)\ S_{31}$	1593	72	12	-108
ARN	1595	135	15	-92
HOE	1608	116	19	-95
CUT	1600$\pm$15	120$\pm$20	15$\pm$2	-110$\pm$20
$\Delta^*(1700)\ D_{33}$	1637	236	16	-38
ARN	1632	253	18	-40
HOE	1651	159	10	
CUT	1675$\pm$25	220$\pm$40	13$\pm$3	-20$\pm$25
$\Delta^*(1910)\ P_{31}$	1840	221	12	-153
ARN	1771	479	45	+172
HOE	1874	283	38	
CUT	1880$\pm$30	200$\pm$40	20$\pm$4	-90$\pm$30

[ARN]: Arndt et al., PRC 74 (2006), [HOE]: Höhler, πN Newsl. 9 (1993), [CUT]: Cutkowski et al., PRD 20 (1979).

Residues to ηN, σN, ρN, $\pi\Delta$. Zeros. Branching ratios to πN, ηN.

Hidden poles in the S_{11} partial wave

[Data: Arndt et al., FA08, EPJA 35 (2008)]

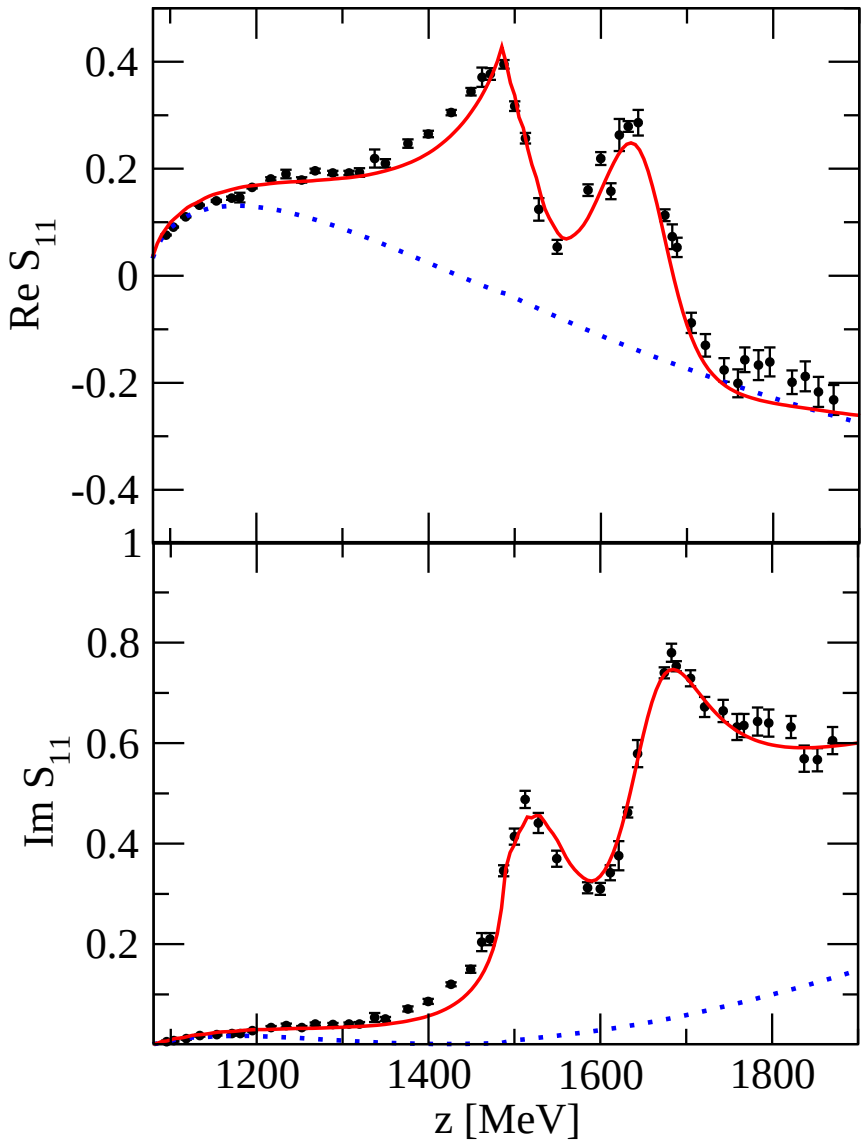

- Laurent series,

$$T^{(2)\,ij} = \frac{a^{ij}_{-1}}{z - z_0} + a^{ij}_0 + \ldots$$

- Resonance interference of $N^*(1535)$ and $N^*(1650)$.

Hidden poles in the S_{11} partial wave

[Data: Arndt et al., FA08, EPJA 35 (2008)]

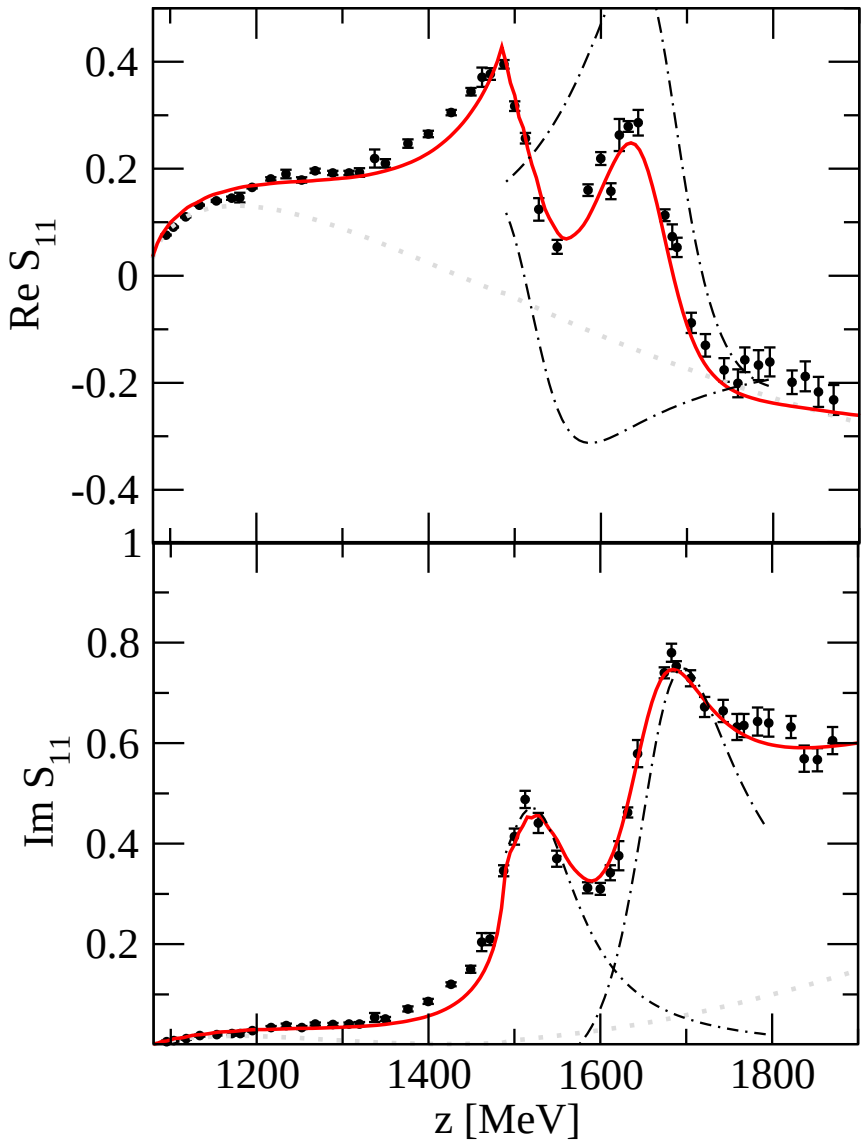

- Laurent series,

$$T^{(2)\,ij} = \frac{a^{ij}_{-1}}{z - z_0} + a^{ij}_0 + \ldots$$

- Resonance interference of $N^*(1535)$ and $N^*(1650)$.

Hidden poles in the S_{11} partial wave

[Data: Arndt et al., FA08, EPJA 35 (2008)]

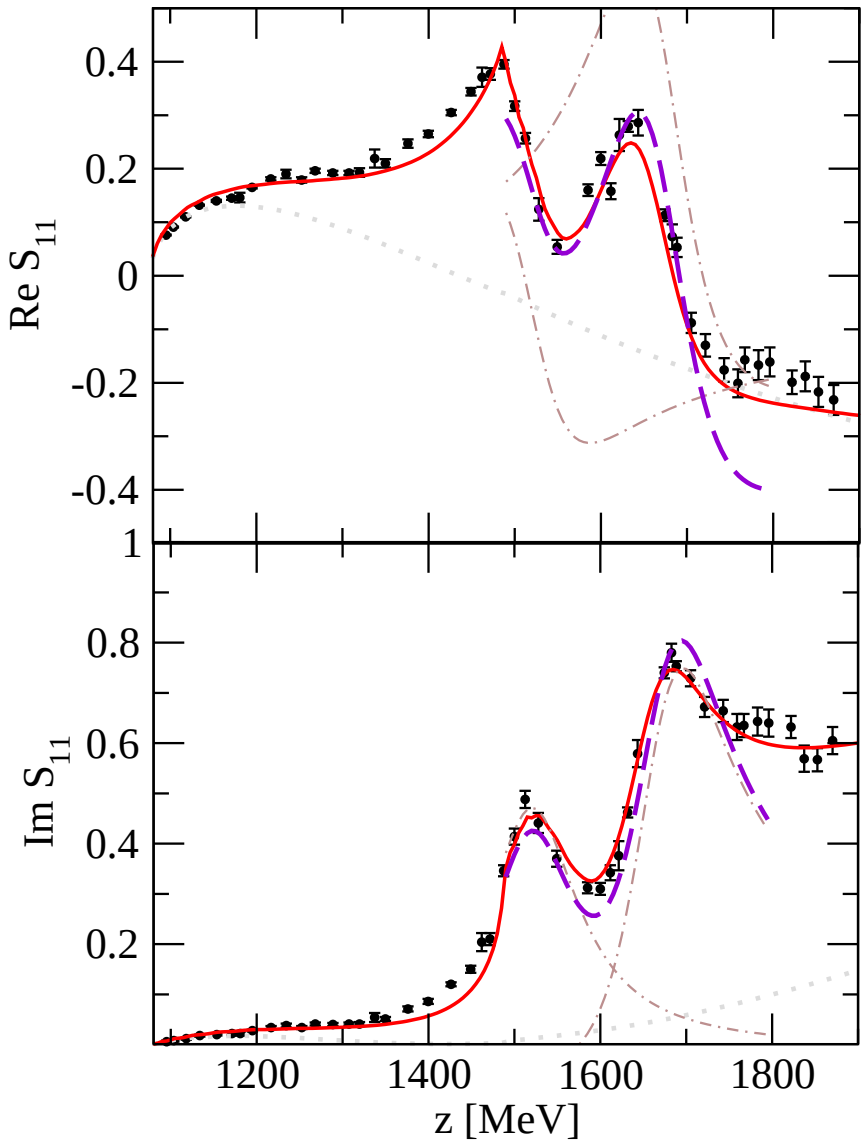

- Laurent series,

$$T^{(2)\,ij} = \frac{a^{ij}_{-1}}{z - z_0} + a^{ij}_0 + \ldots$$

- Resonance interference of $N^*(1535)$ and $N^*(1650)$.

Hidden poles in the S_{11} partial wave

[Data: Arndt et al., FA08, EPJA 35 (2008)]

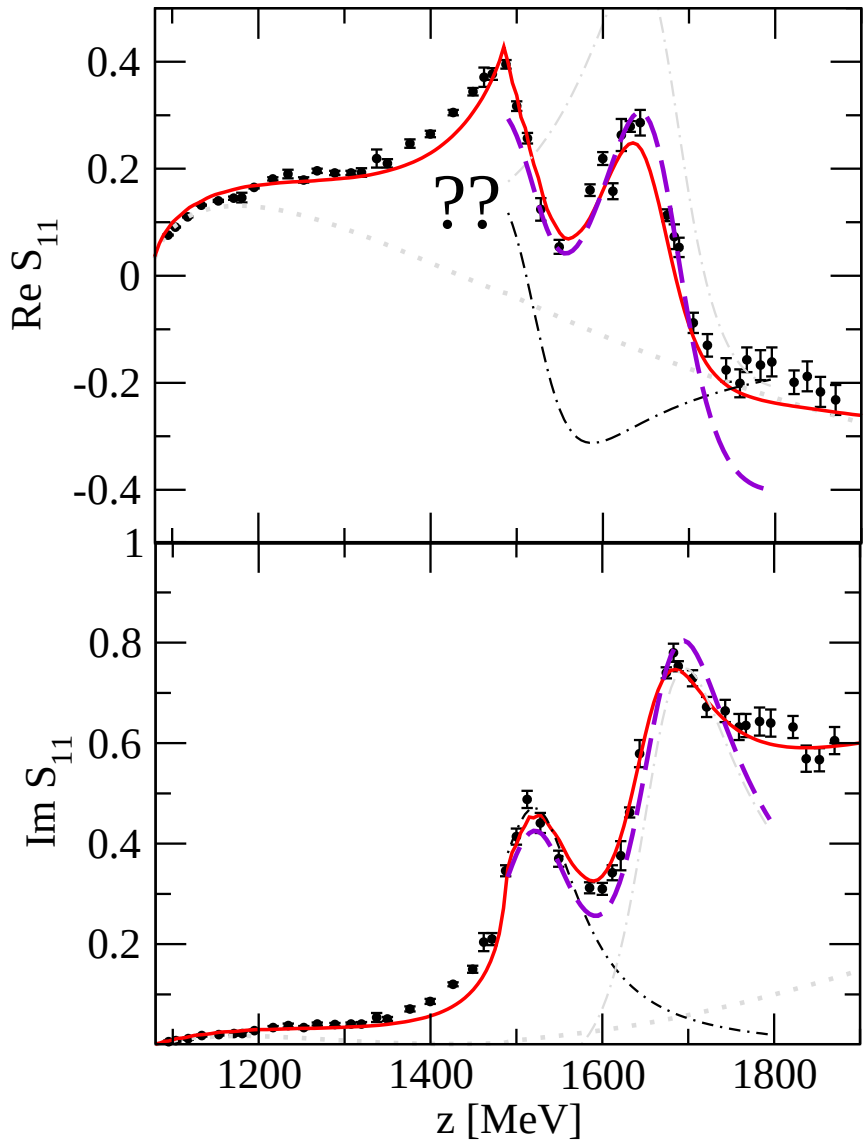

- Laurent series,

$$T^{(2)\,ij} = \frac{a^{ij}_{-1}}{z - z_0} + a^{ij}_0 + \ldots$$

- Resonance interference of $N^*(1535)$ and $N^*(1650)$.

Hidden poles in the S_{11} partial wave

[Data: Arndt et al., FA08, EPJA 35 (2008)]

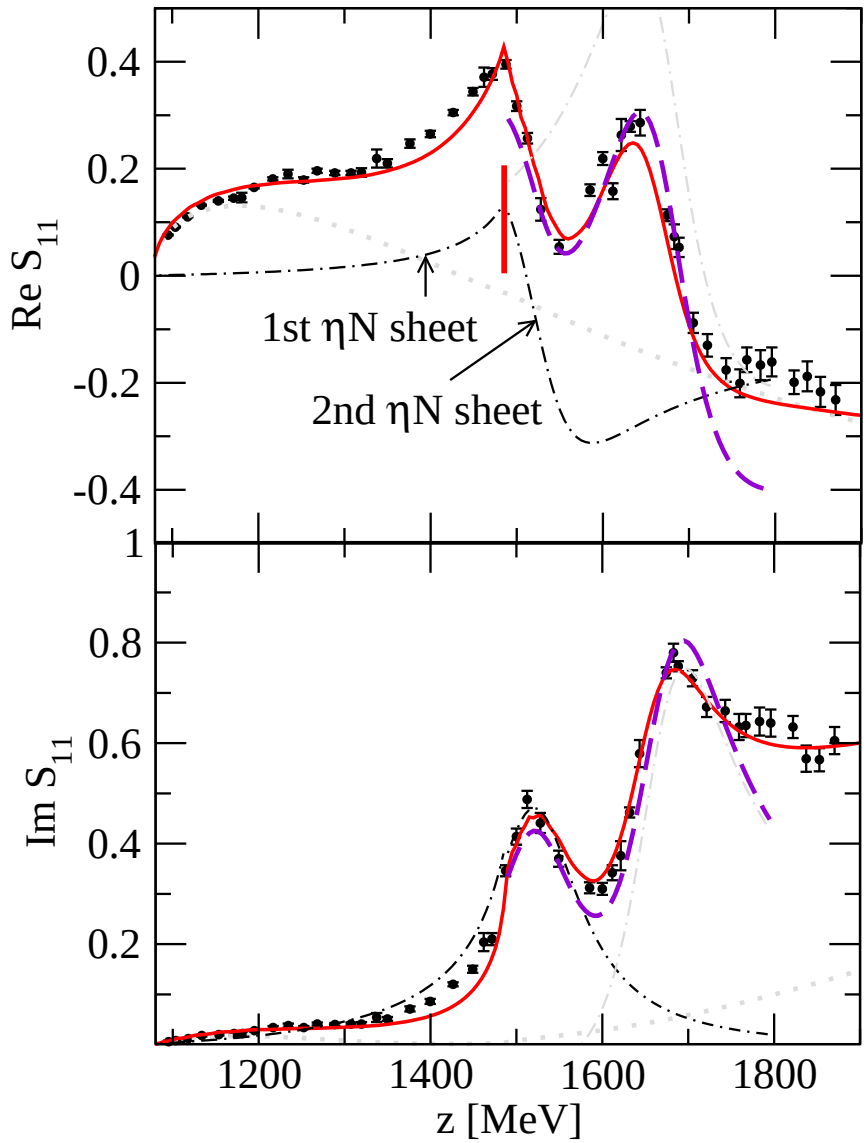

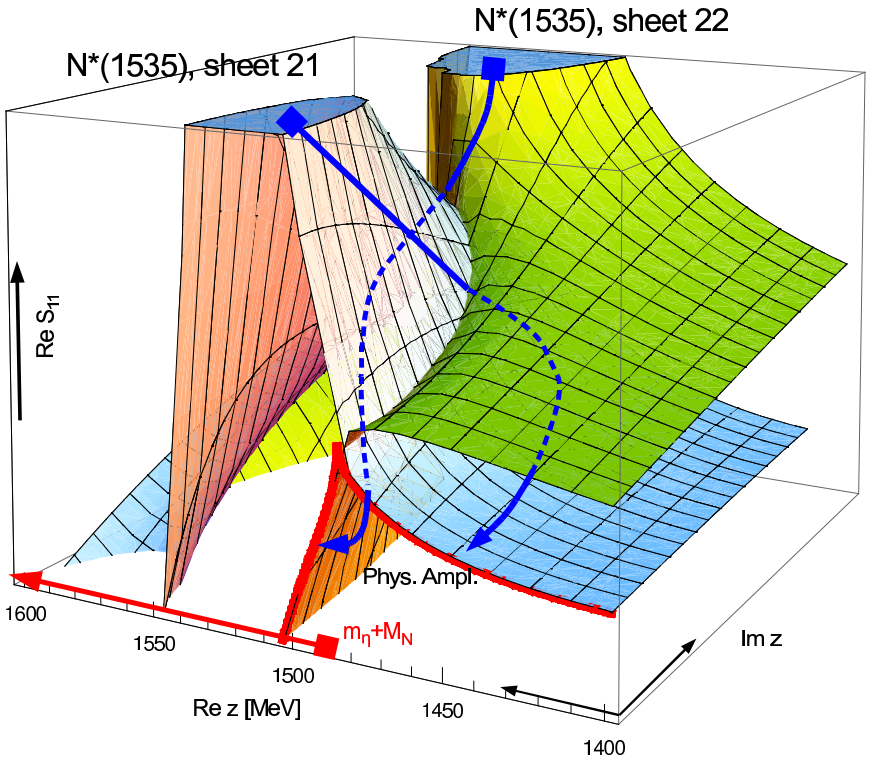

- Different poles on different sheets produce the cusp.
- → Two-pole structure! (x2 resonances)

Hidden poles in the S_{11} partial wave

[Data: Arndt et al., FA08, EPJA 35 (2008)]

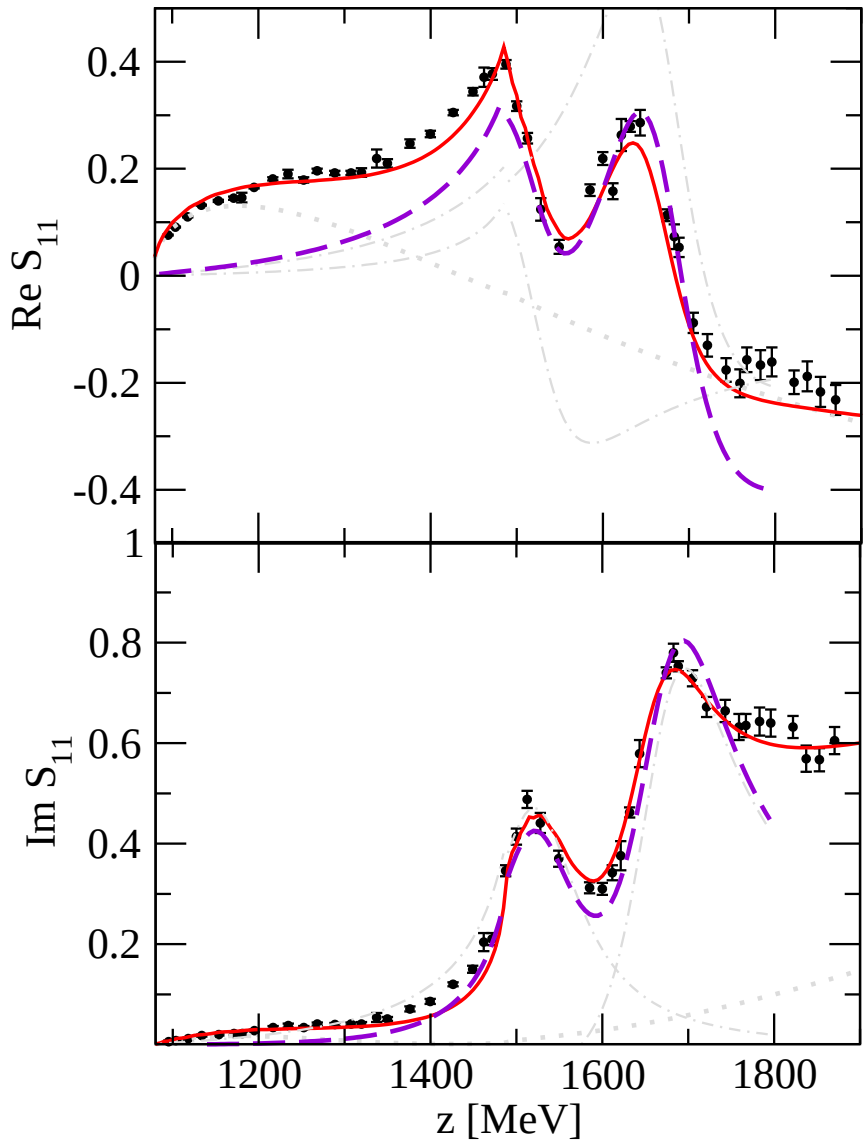

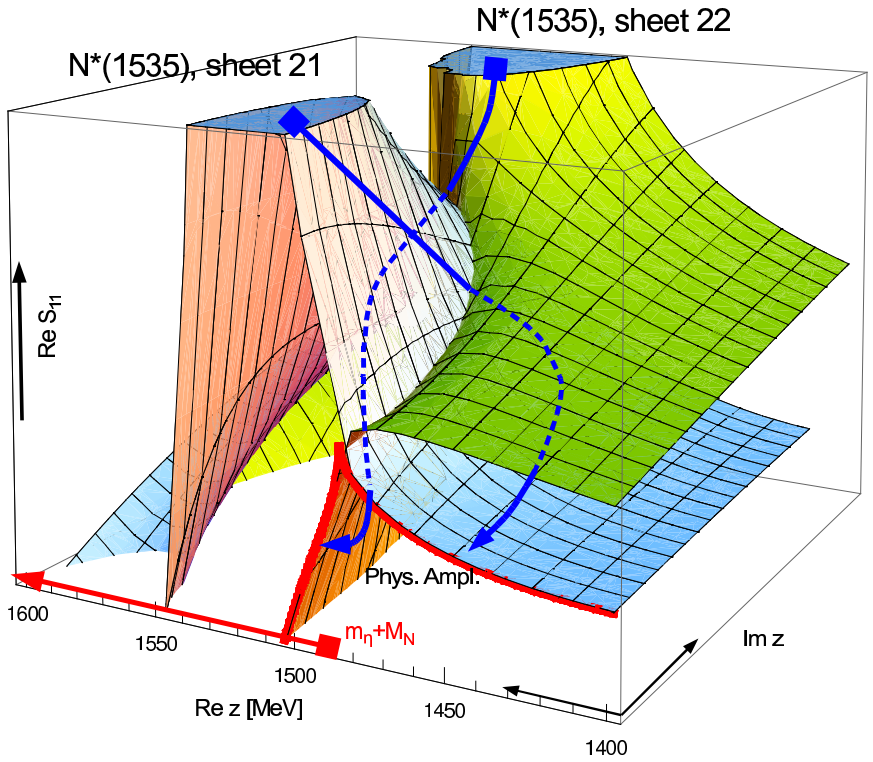

- Different poles on different sheets produce the cusp.
- → Two-pole structure! (x2 resonances)

The two poles of the Roper resonance

- SAID/EBAC/Jülich: PRC 69 (2004)/ PRC 79 (2009); arXiv:0909.1356 (2009)/ NPA 829 (2009)] two poles of the Roper, in all cases on two different $\pi\Delta$ sheets.
- Poles on hidden sheets can be only seen through the corresponding branch point $\Rightarrow$ Structures from hidden poles appear as...
  - ... cusps if branch point on physical axis ($N(1535)$ case close to ηN threshold)
  - ... washed out cusps (non-standard resonance shape) if branch point in the complex plane (Roper case close to $\pi\Delta$ threshold).
- Proposed two-pole structure of the $\Lambda(1405)$ [Jido et al., NPA 725 (2003); M.D. et al. EPJA 32 (2007)]: both poles on same, non-hidden, sheet $\rightarrow$ experimental tests may be possible.

An additional state in P11

* New pole in P11 found
  at z=1620 + 297 i MeV.

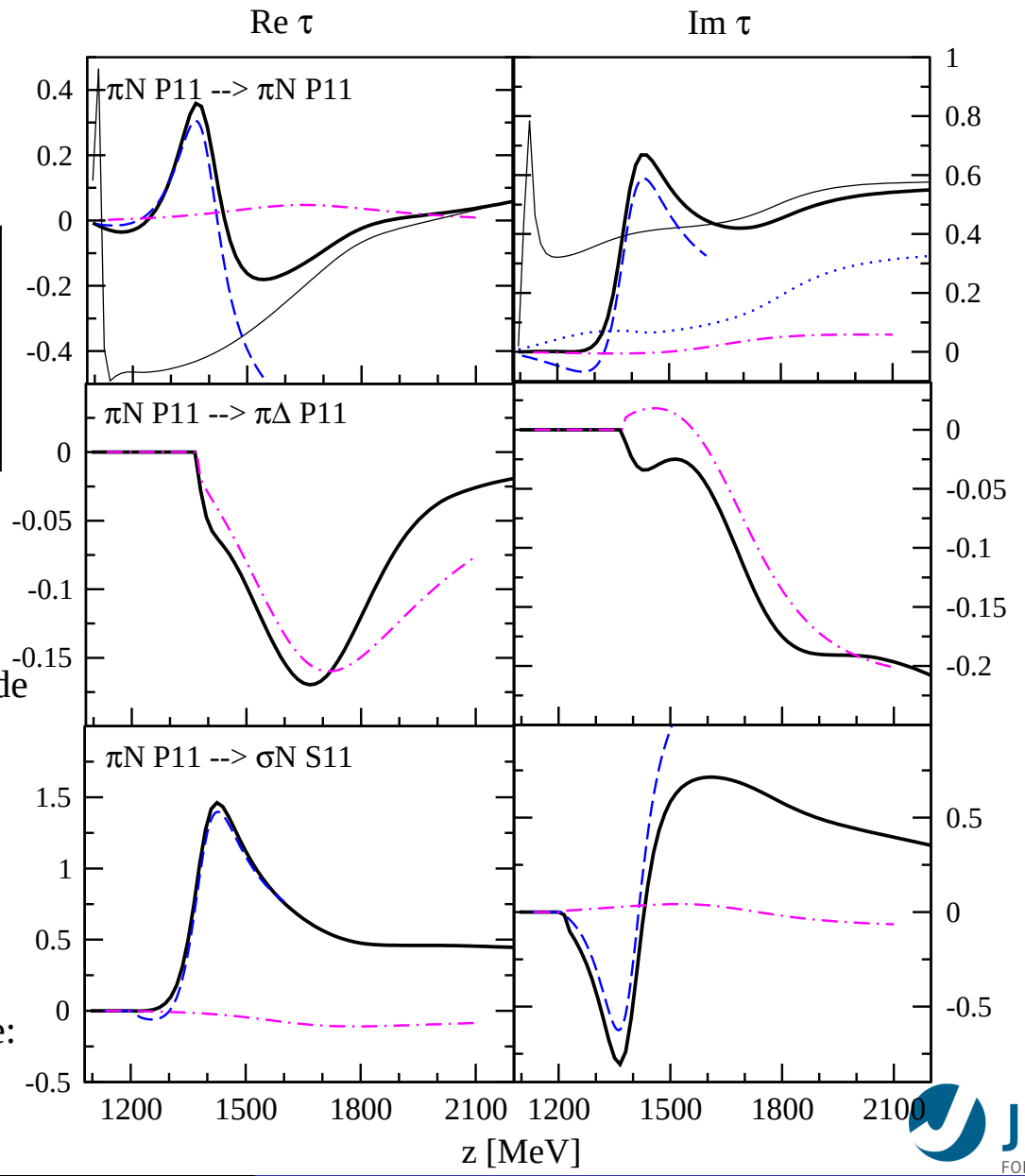

* Very weak branching to πN.
* Very large branching to πΔ.
* Resonance transition amplitude
  πN --> πΔ:
  Manley (πN --> ππN): -0.21
  here: -0.25

* Roper: generated from σN.
* N(1620): generated from πΔ.

* Dynamics of the nucleon pole:
  Pole repulsion N <--> Roper

Pole repulsion in P_{33}

Situation in D13

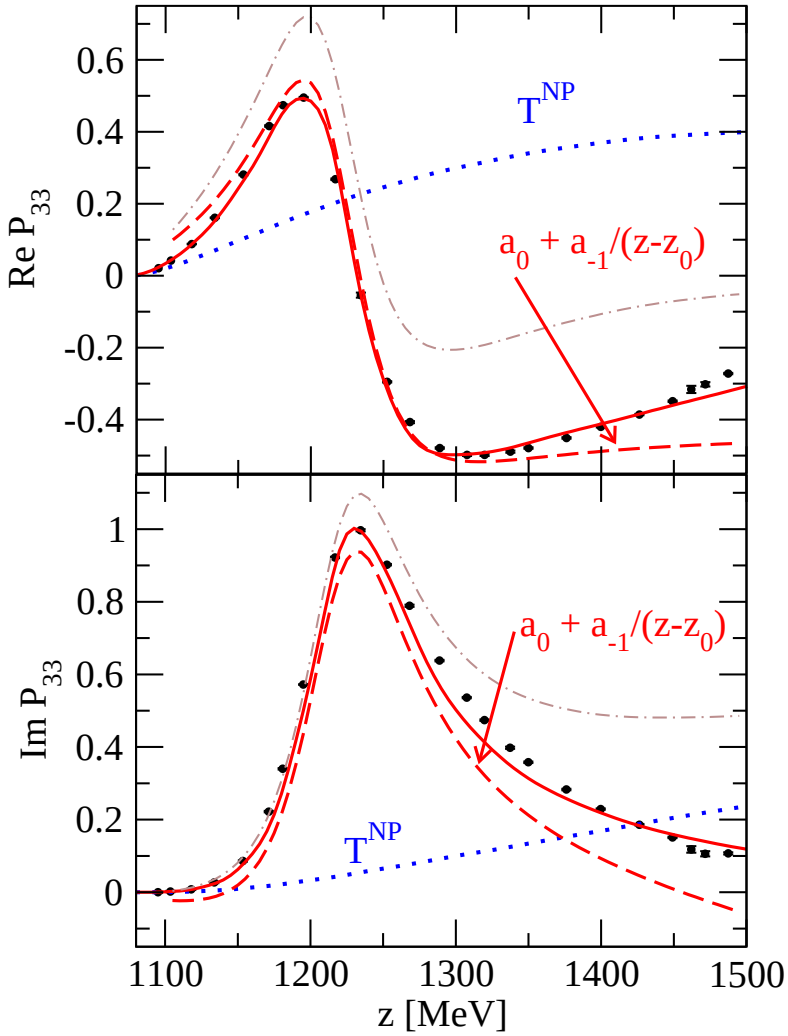

- Poles in T^{NP} may occur $\Rightarrow$ pole repulsion in $T = T^{\mathrm{NP}} + T^{\mathrm{P}}$!

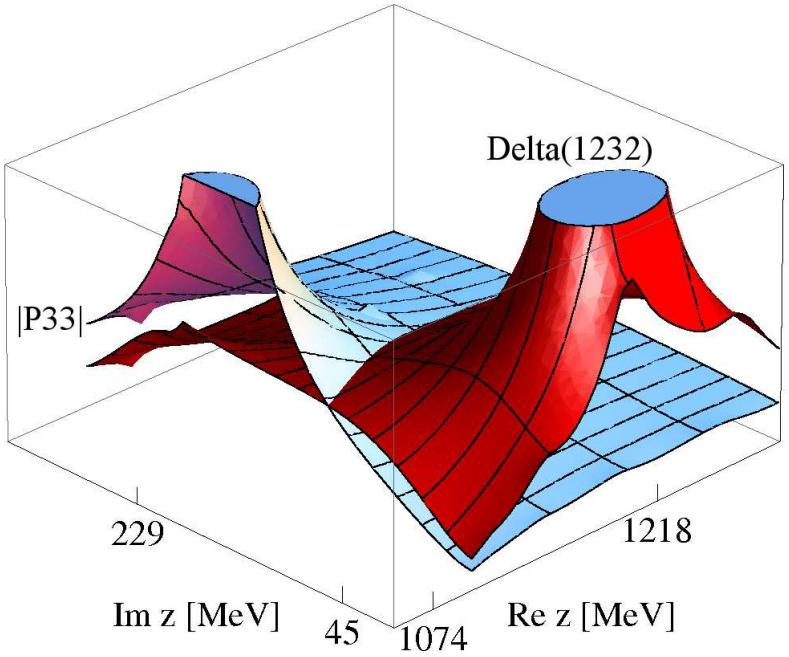

- Back to P11:
  - T^{P} given by renormalized/dressed nucleon.
  - Roper: pole in T^{NP}.
  - $T = T^{\mathrm{NP}} + T^{\mathrm{P}}$: Roper is moved to physical position; N $\leftrightarrow$ Roper repulsion.

Summary: The analytic structure of the P11 partial wave

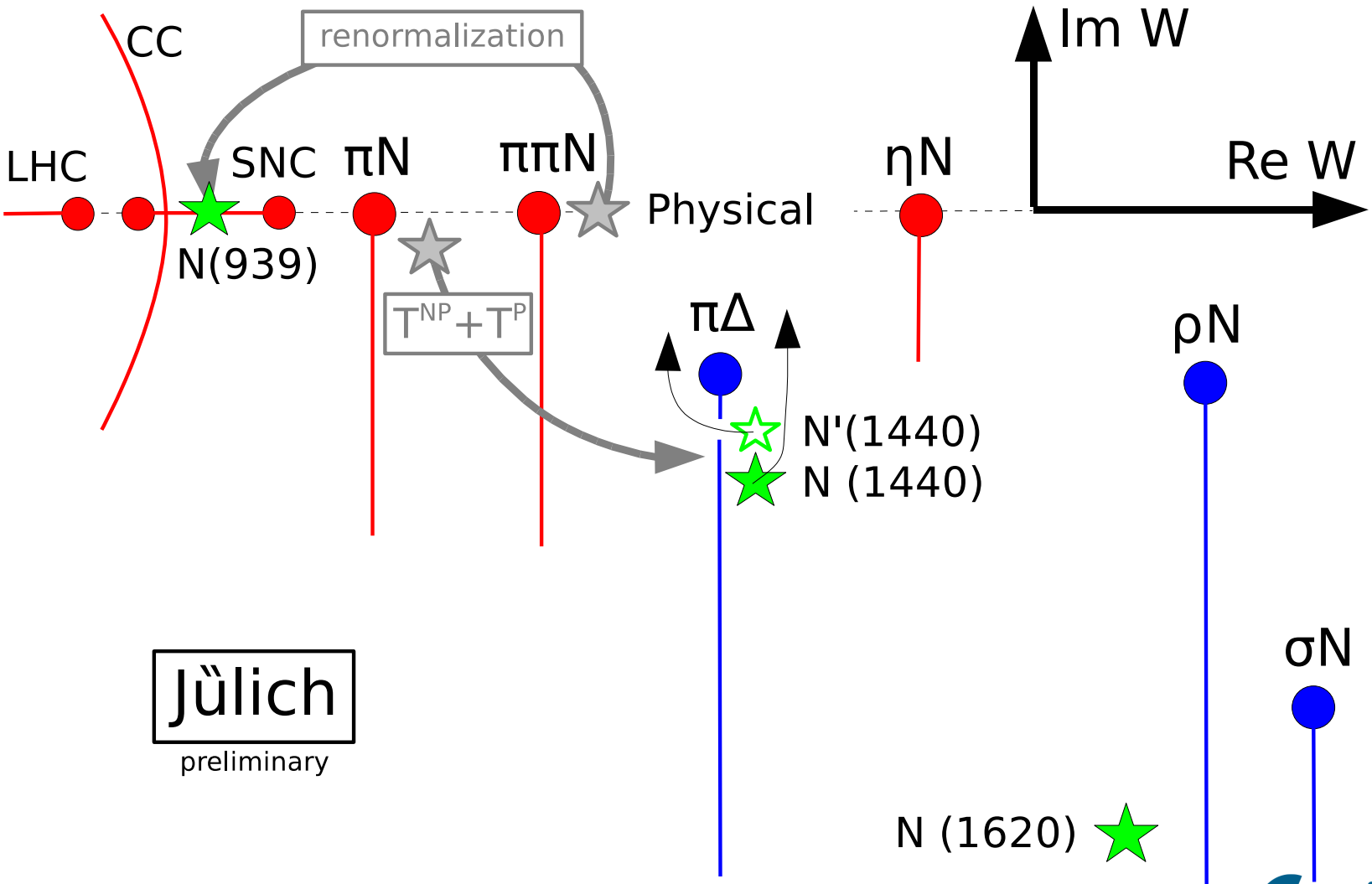

Jülich
preliminary

Summary: The analytic structure of the P11 partial wave

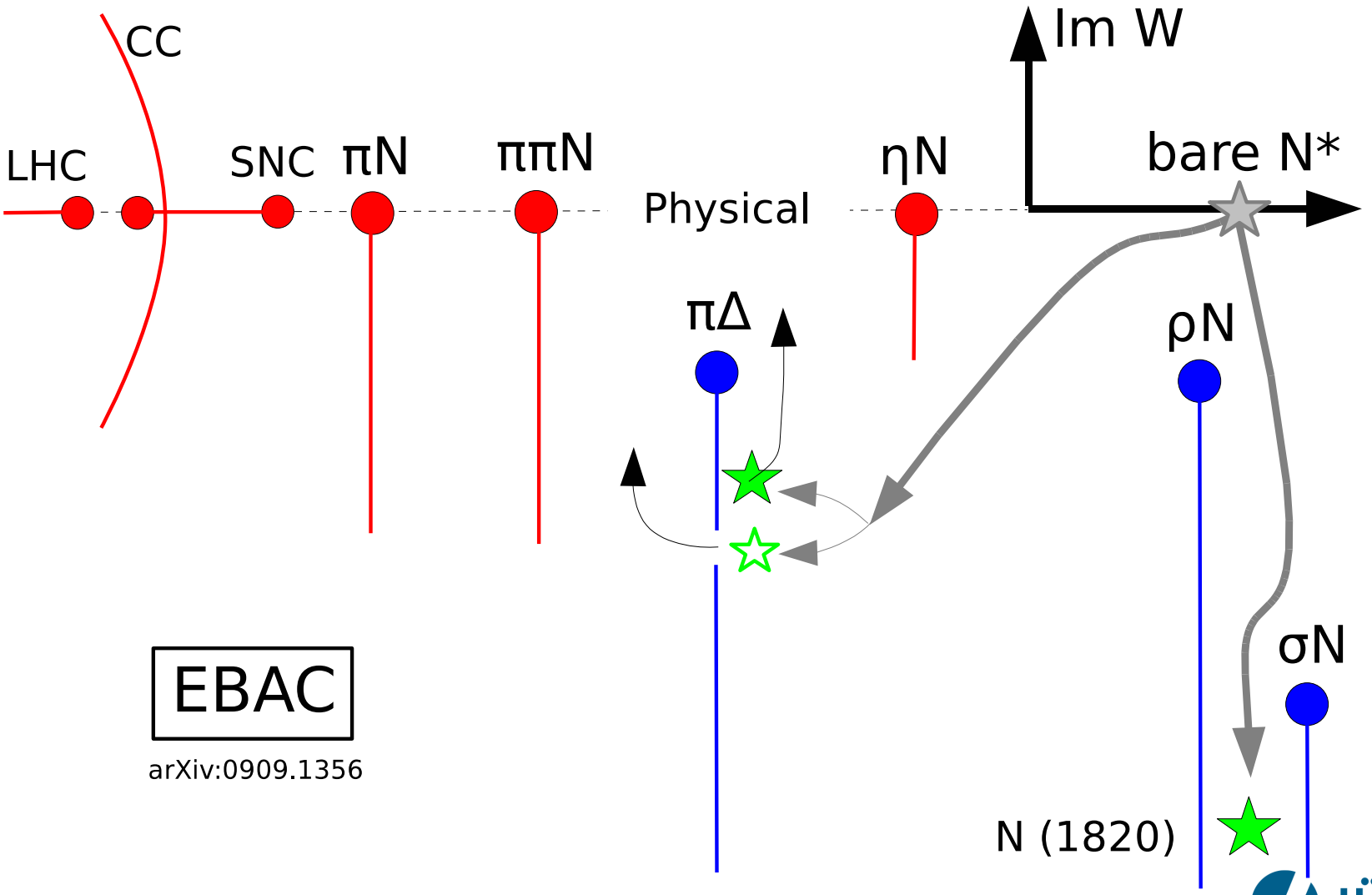

Outlook: Matching with lattice results

- Pole position is quark mass dependent, Re $\Sigma(m_\pi)$.
- Quark mass dependence of effective $2\pi N$ channels (to be done).
- Analytic model allows for matching with lattice results ($m_\pi >> m_\pi^{\text{phys.}}$).

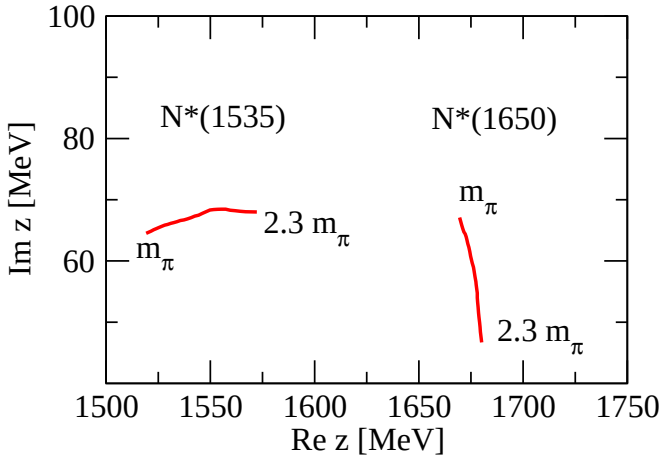

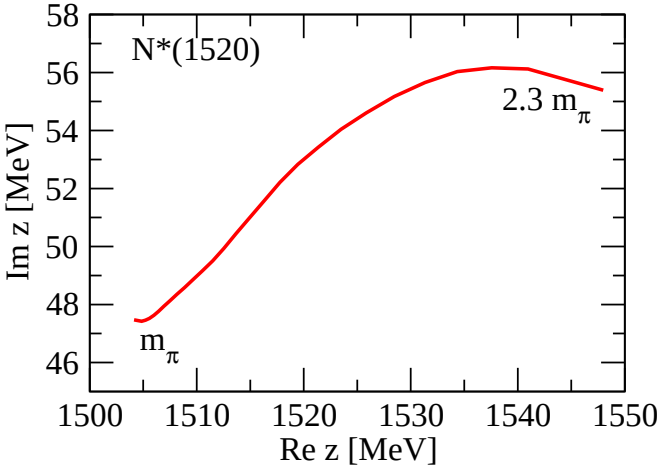

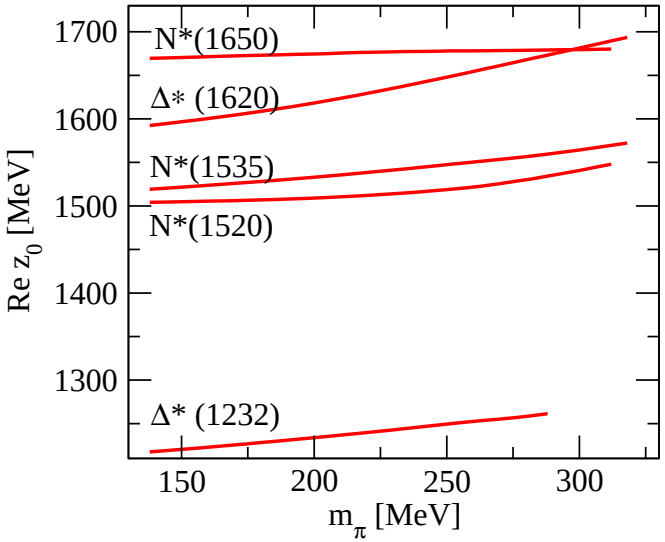

Conclusions

- First results for the photoproduction have been obtained.
- Gauge invariant amplitude.
- The analytic continuation allows to access the sheets of the amplitude in the complex plane.
- Poles are found (in particular the dynamically generated Roper).
  - Positions.
  - Residue strengths and angles.
- Structure of the P11 amplitude.
  - Nucleon renormalized to its physical properties (is the only genuine pole term in $P11$).
  - Roper dynamically generated mainly from σN channel.
  - Two poles of the Roper resonance, but on different sheets.
  - An additional state at $W = 1620$ MeV far in the complex plane, generated mainly from $\pi\Delta$; shares properties of the $N(1710)\,P_{11}$.
  - Resonance interference ("pole repulsion") between nucleon and Roper throgh intermediate states is important for the dynamics.
  - Caution when identifying T^{NP} as "background". T^{NP} is model dependent; $T = T^{\mathrm{P}} + T^{\mathrm{NP}}$ is physically meaningful.

Current and future projects

- π and η photo- and Electroproduction.
- $\pi\pi N$ production.
- Inclusion of higher spin resonances ($J > 3/2$).
- Inclusion of KY channels.
- Conceptual improvements: Consistent treatment of three-body cuts; three-body unitarity.
- Conceptual improvements: Matching to chiral perturbation theory.

Couplings " $g = \sqrt{a_{-1}}$ " to other channels

back

	$N\pi$	$N\rho^{(1)}$ $(S=1/2)$	$N\rho^{(2)}$ $(S=3/2)$	$N\rho^{(3)}$ $(S=3/2)$
$N^*(1535)\,S_{11}$	S_{11} $8.1+0.5i$	S_{11} $2.2-5.4i$	$-$	D_{11} $0.5-1.3i$
$N^*(1650)\,S_{11}$	S_{11} $8.6-2.8i$	S_{11} $0.9-9.1i$	$-$	D_{11} $0.3-2.0i$
$N^*(1440)\,P_{11}$	P_{11} $11.2-5.0i$	P_{11} $-1.3+3.2i$	P_{11} $3.6-2.6i$	$-$
$\Delta^*(1620)\,S_{31}$	S_{31} $2.9-3.7i$	S_{31} $0.0-0.0i$	$-$	D_{31} $0.0+0.5i$
$\Delta^*(1910)\,P_{31}$	P_{31} $1.2-3.5i$	P_{31} $0.2-0.4i$	P_{31} $-0.2-0.4i$	$-$
$N^*(1720)\,P_{13}$	P_{13} $3.7-2.6i$	P_{13} $0.1+0.8i$	P_{13} $-1.1+0.1i$	F_{13} $0.1+0.4i$
$N^*(1520)\,D_{13}$	D_{13} $8.4-0.8i$	D_{13} $-0.6+0.7i$	D_{13} $0.9-2.0i$	S_{13} $-2.5-22.8i$
$\Delta(1232)\,P_{33}$	P_{33} $17.9-3.2i$	P_{33} $-1.3-0.8i$	P_{33} $-0.9-3.0i$	F_{33} $0.0-0.0i$
$\Delta^*(1700)\,D_{33}$	D_{33} $4.9-1.0i$	D_{33} $-0.2+0.9i$	D_{33} $-0.4-0.4i$	S_{33} $-0.1-0.9i$

	$N\eta$	$\Delta\pi^{(1)}$	$\Delta\pi^{(2)}$	$N\sigma$
$N^*(1535)\,S_{11}$	S_{11} $11.9-2.3i$	$-$	D_{11} $-5.9+4.8i$	P_{11} $-1.4-1.2i$
$N^*(1650)\,S_{11}$	S_{11} $-3.0+0.5i$	$-$	D_{11} $4.3+0.4i$	P_{11} $-2.1-1.0i$
$N^*(1440)\,P_{11}$	P_{11} $-0.1+0.0i$	P_{11} $-4.6-1.7i$	$-$	S_{11} $-8.3-27.7i$
$\Delta^*(1620)\,S_{31}$	$-$	$-$	D_{31} $11.1-4.0i$	$-$
$\Delta^*(1910)\,P_{31}$	$-$	P_{31} $15.0-0.3i$	$-$	$-$
$N^*(1720)\,P_{13}$	P_{13} $-7.7+5.5i$	P_{13} $-14.1+3.0i$	F_{13} $0.0-0.3i$	D_{13} $-0.8+0.4i$
$N^*(1520)\,D_{13}$	D_{13} $0.16-0.60i$	D_{13} $0.0+0.4i$	S_{13} $-12.9-0.7i$	P_{13} $-0.6-0.6i$
$\Delta(1232)\,P_{33}$	$-$	P_{33} $-(4\text{ to }5)+i(0\text{ to }0.5)$	F_{33} ~ 0	$-$
$\Delta^*(1700)\,D_{33}$	$-$	D_{33} $-0.7-0.3i$	S_{33} $-19.7+4.5i$	$-$

Resonance couplings g_i $[10^{-3}\,\mathrm{MeV}^{-1/2}]$ to the coupled channels i. Also, the LJS type of each coupling is indicated. For the ρN channels, the total spin S is also indicated.

Zeros and branching ratio to πN, ηN

back

first sheet		second sheet		[FA02]
P_{11}	$1235 - 0\,i$	S_{11}	$1587 - 45\,i$	$1578 - 38\,i$
D_{33}	$1396 - 78\,i$	S_{31}	$1585 - 17\,i$	$1580 - 36\,i$
		P_{31}	$1848 - 83\,i$	$1826 - 197\,i$
		P_{13}	$1607 - 38\,i$	$1585 - 51\,i$
		P_{33}	$1702 - 64\,i$	–
		D_{13}	$1702 - 64\,i$	$1759 - 64\,i$

Position of zeros of the full amplitude T in [MeV]. [FA02]: Arndt et al., PRC 69 (2004).

	$\Gamma_{\pi N}/\Gamma_{\rm Tot}$ [%]	$\Gamma_{\eta N}/\Gamma_{\rm Tot}$ [%]
$N^*(1535)\,S_{11}$	48 [33 to 55]	38 [45 to 60]
$N^*(1650)\,S_{11}$	79 [60 to 95]	6 [3 to 10]
$N^*(1440)\,P_{11}$	64 [55 to 75]	0 [0 ± 1]
$\Delta^*(1620)\,S_{31}$	34 [20 to 30]	–
$\Delta^*(1910)\,P_{31}$	11 [15 to 30]	–
$N^*(1720)\,P_{13}$	13 [10 to 20]	38 [4 ± 1]
$N^*(1520)\,D_{13}$	67 [55 to 65]	0.10 [0.23 ± 0.04]
$\Delta(1232)\,P_{33}$	100 [100]	–
$\Delta^*(1700)\,D_{33}$	13 [10 to 20]	–

Branching ratios into πN and ηN. The values in brackets are from the PDG, [Amsler et al., PLB 667 (2008)].

Couplings and dressed vertices

back

Residue a_{-1} vs. dressed vertex Γ vs. bare vertex γ.

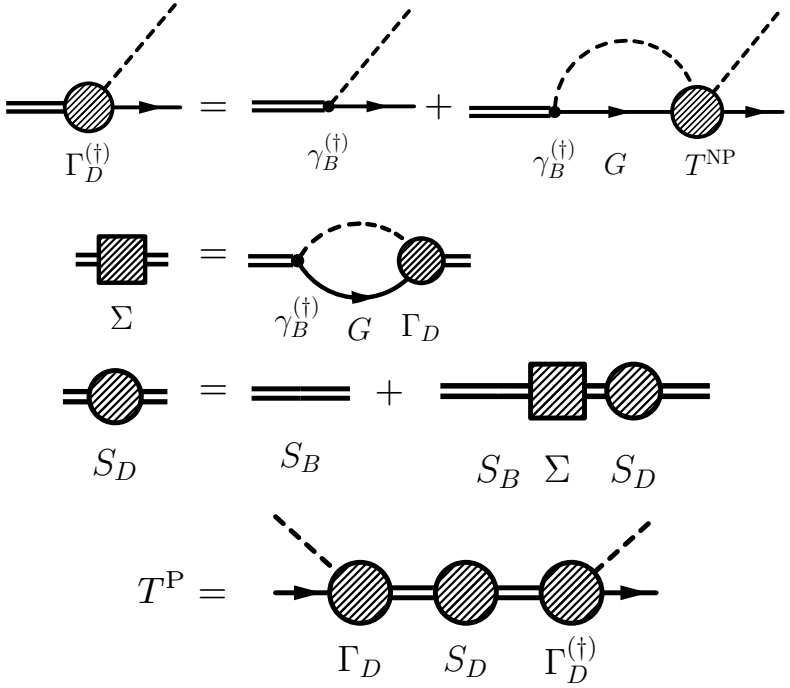

$$
\begin{aligned}
a_{-1} &= \frac{\Gamma_d\,\Gamma_d^{(\dagger)}}{1-\frac{\partial}{\partial Z}\Sigma} \\
g &= \sqrt{a_{-1}} \\
r &= |(\Gamma_D-\gamma_B)/\Gamma_D|, \\
r' &= |1-\sqrt{1-\Sigma'}|,
\end{aligned}
$$

- Dressed Γ depends on $T^{\rm NP}$.
- $\boxed{\sqrt{a_{-1}} \neq \Gamma \neq \gamma}$

	γ^C	Γ^C	r [%]	r' [%]
$N^*(1520)\,D_{13}$	$6.4-0.6i$	$13.2+1.2i$	53	61
$N^*(1720)\,P_{13}$	$-0.1+5.4i$	$0.9+4.8i$	24	45
$\Delta(1232)\,P_{33}$	$1.3+13.0i$	$-2.8+22.2i$	45	40
$\Delta^*(1620)\,S_{31}$	$0.1+14.3i$	$5.0+5.7i$	130	66
$\Delta^*(1700)\,D_{33}$	$5.4-0.8i$	$6.7+1.0i$	33	54
$\Delta^*(1910)\,P_{31}$	$9.4+0.3i$	$1.9-3.2i$	222	22

The D_{13} partial wave

back

The $N^*(1520)$ and a dynamically generated pole in T^{NP}.

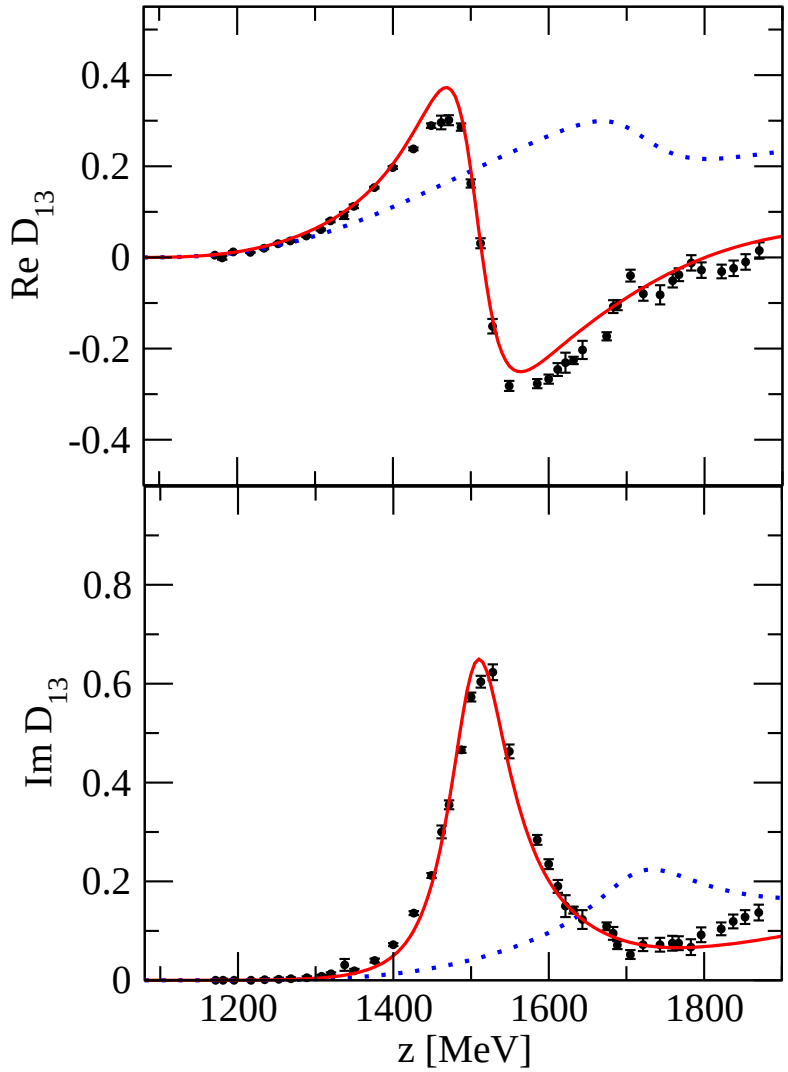

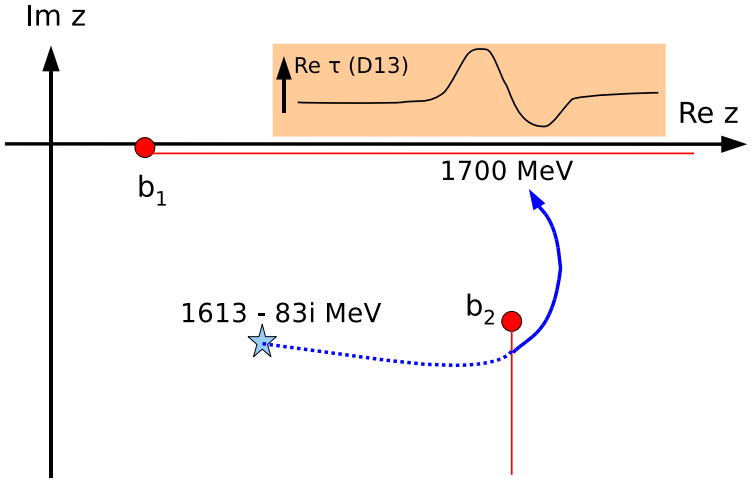

- T^{NP}: no s-channel $N^*(1520)$.
- Pole in T^{NP} on 3rd ρN sheet.
- On physical axis visible through branch point b_2.
- Pole invisible in full solution. $\longrightarrow$ We do not identify it with a dynamically generated $N^*(1700)$.

[Ramos, Oset, arXiv:0905.0973 [hep-ph]]